DEVELOPMENT OF FINITE ELEMENT MODEL FOR ANALYSIS OF PRESTRESSED CONCRETE CYLINDER PIPE-EMBEDDED CYLINDER PIPE WITH EXPERIMENTAL COMPARISON

by

SANGIT RAUNIYAR

Presented to the Faculty of the Graduate School of

The University of Texas at Arlington in Partial Fulfillment

of the Requirements

for the Degree of

MASTER OF SCIENCE IN CIVIL ENGINEERING

THE UNIVERSITY OF TEXAS AT ARLINGTON

May 2013

ACKNOWLEDGEMENTS

I would like to express my sincere thanks to Prof. Dr. Ali Abolmaali for his guidance and remarkable patience throughout the supervision of this research and providing valuable suggestions and corrections during the research work, and preparation and completion of my thesis.

I would like to extend my appreciation to Dr. Siamak Ardekani and Dr. Shih-Ho Chao for their comments and suggestions for this study.

I would like to thank Sam Aranout and Wu Ricky for their help and suggestions during the research work. Also, I would like to thank Joe Lundy and Josh Beakley for providing invaluable input in understanding the pipe behavior, in general.

I appreciate Tarrant Regional Water District for their financial assistance for this research project. Also, I am grateful to Hanson Pipe and Precast for their support in conducting the research project.

Finally, I thank my parents, who are in Nepal, and my family here, in USA, for their support. I also extend my appreciation to Mojtaba S. Dezfooli and Dr. Yeonho Park without whom the completion of this thesis was not possible.

April 22, 2013

ABSTRACT

DEVELOPMENT OF FINITE ELEMENT MODEL FOR ANALYSIS OF PRESTRESSED CONCRETE CYLINDER PIPE-EMBEDDED CYLINDER PIPE WITH EXPERIMENTAL COMPARISON

Sangit Rauniyar, M.S.

The University of Texas at Arlington, 2013

Supervising Professor: Ali Abolmaali

Prestressed Concrete Cylinder Pipe (PCCP) is a composite pipe that consists of concrete and steel, which has layers of concrete core, steel cylinder, prestressing wire and mortar coating. PCCP is generally constructed of two types; a steel cylinder lined with a concrete core and a steel cylinder embedded in a concrete core. The former type is called PCCP-Lined Cylinder Pipe (PCCP-LCP) and the latter type is called PCCP-Embedded Cylinder Pipe (PCCP-ECP). The scope of this paper is limited to PCCP-ECP.

PCCP-ECP is a composite material with complex stress phenomenon due to prestress and interaction between different layers of components. A three dimensional non-linear finite element model is generated by using Abaqus version 6.12-2, a program that is well suited for non-linear finite element modeling, to simulate the real pipe behavior. The PCCP-ECP is modeled by considering the contribution of each components and manufacturing process. The hexahedron mesh, which is popular for accuracy and convergence, is used to model the elements. The simultaneous effect of shrinkage, creep, and relaxation are considered. Negative

temperature is applied to simulate the shrinkage and creep of concrete. Also, time dependent property is defined to simulate the relaxation of prestressing wire.

Two full scale experiments, three edge bearing tests, were conducted to determine the real ECP behavior. The three edge bearing test was also simulated by using three dimensional non-linear analysis on the modeled PCCP-ECP. The comparison of results obtained from experiment and finite element modeling is done, which shows good agreement between the results. The PCCP-ECP model can be used for analysis for any loading case.

TABLE OF CONTENTS

LIST OF ILLUSTRATIONS

Figure Page

LIST OF TABLES

Table Page

CHAPTER 1

INTRODUCTION AND LITERATURE REVIEW

Prestressed Concrete Cylinder pipe-Embedded Cylinder Pipe (PCCP-ECP) is custom designed pipe. It is practically infeasible to conduct experiment on PCCP-ECP for each project. Therefore, a non-linear three-dimensional finite element is needed for detail analysis of PCCP-ECP. The objective of this research is to develop a non-linear three-dimensional model of PCCP-ECP that considers simultaneous effect of shrinkage, creep, and relaxation as well as non-linearities due to geometry, material, and contact. Also, two full scale experiments were conducted to validate the model by comparing behavior of model with real PCCP-ECP.

1.1 Concrete Pressure Pipe

According to American Concrete Pressure Pipe Association (ACPPA), “concrete pressure pipe is an engineered product that combines the best features of Portland cement concrete and steel to create a robust structure for conveying liquids within a wide range of external loads and internal pressures.” There are several advantages of concrete pressure pipe: durable; economical; adaptable; reliable; sustainable; and certified quality.

Concrete pressure pipe is durable because it is able to handle a wide range of external loads and internal pressures. It is easy to install and maintenance cost is very small, which makes it more economical. Unlike other pipes, concrete pressure pipe is custom designed for each project, which allows it to fulfill the requirement of each project. Also, concrete pressure pipe is being used for last 100 years, and it has shown the acceptable performance. In addition, ACPPA’s annual audit program, which is administered by Lloyd’s Register Quality Assurance

(LRQA), ensures the production of concrete pressure pipe is in compliance with American Water Works Association (AWWA) standards.

Concrete pressure pipes are classified as follows: reinforced concrete pressure pipe, steel cylinder type (AWWA C300); reinforced concrete pressure pipe, non-cylinder type(AWWA C302); concrete pressure pipe, bar-wrapped, steel cylinder type (AWWA C303); and Prestressed concrete pressure pipe, steel-cylinder type (PCCP, AWWA C301).

1.2 History of concrete pressure pipe and development of PCCP

According to Whitlock (1960), the Romans constructed several concrete water lines, and some of these pipes were in service for many centuries. In the United States, first concrete pressure pipe was used for irrigation in the West. Between 1870 and 1900, concrete pressure pipe were considerably used and developed in New England. It consisted of sheet of wrought iron, lapped and riveted to form a cylinder and covered inside and outside with natural cement mortar. The interior cement mortar core was placed by rolling or revolving the cylinder at a relatively low speed. The exterior mortar was generally applied in the trench by placing a layer in the bottom and shaping it around the pipe by hand. Experience in use of this kind of pipe probably was a factor in the later development of steel cylinder concrete pressure pipe.

The first reinforced concrete cylinder pressure pipeline was a 36 inch line constructed at Cumberland, Md., in 1919. In the Western and Southwestern United States, a kind of concrete pressure pipe generally known as pretensioned concrete cylinder pipe had been used extensively for several years. Another type, which had been used principally for low-pressure lines, is non-cylinder concrete pressure pipe that is not prestressed. From 1920 to 1940, most of the concrete pressure pipe used in the United States by water supply industry was steel cylinder concrete pipe, which was not prestressed.

Also, in 1942 the concept of pre-stressing of concrete pipe emerged. During the World War II, the American Pipe and Construction Company (Ameron) faced with wartime shortages

came up with the idea of combining available thinner steel material with rod wrap in lieu of cylinder alone for pressure pipes, which leads to the development of bar-wrapped pipe. However, to save more steel, the concept of increasing wall thickness of pipe and using thinner steel emerged for pressure pipes. In 1942, Prestressed Concrete Cylinder Pipe (PCCP) was built and named it as lined PCCP (PCCP-LCP), and it was installed in the USA for the first time. In PCCP-LCP steel cylinder was lined with concrete core, and pre-stressing wire is wrapped on the steel cylinder. Also, in 1952 the concept of embedding the thin steel cylinder inside concrete core in PCCP emerged that leads to production of new type of PCCP called embedded PCCP (PCCP-ECP).

PCCP is used as pressure pipe for the purpose of transmission mains, distribution feeder mains, water intake and discharge lines, pressure siphons, low-head penstocks, industrial pressure lines, power plant cooling-water lines, sewer force mains, subaqueous lines, and spillway conduits. The typical diameter ranges for LCP and ECP are 16 to 60 inches and 30 to 256 inches respectively. The design and manufacturing standards for PCCP was first developed in 1942, which was later approved by AWWA in 1949. The AWWA C301, standard for PCCP, steel cylinder type, was first published in 1952. Although LCP was first installed in the USA in 1942, ECP was first installed in the USA in 1953. In 1958, second edition of AWWA C301 was published, which changed the allowable stress in wire from 45% to 70% of ultimate strength, and minimum mortar thickness from 7/8 inch to 5/8 inch. The earlier design and manufacturing of PCCP were relatively expensive due to conservative high safety factors in design. However, due to continuous research in understanding behavior of PCCP and advancement of material science, it has now become economical. In addition to this, advancement of steel industries has also played crucial role in manufacturing of effective PCCP. For example, in late 1960's and early 1970's , high tensile strength steel wire were developed, which reduced the amount of pre-stressing wire required for the same prestressing force. As a result industries were able to use thin wires, such as class IV wire. In 1964, third

edition of AWWA C301 was published, which changed the allowable wire stress to 75% of ultimate strength. According to Romer (2007) and Romer et al. (2008), pipe from this era started failing before design life. AWWA C301 was again revised in 1972 and in 1979. Also, in 1979, Manual M9, manual of concrete pressure pipe, was published. In 1984, AWWA C301 was revised, which changed the minimum coating requirement to 3/4 inch, and cast concrete coating was removed. In 1992, major changes were done in the PCCP standard: the appendices were deleted; minimum wire size increased to 0.192 inch; minimum cylinder thickness increased to 16 gauge; AWWA C304 was published. In 1995, second edition of Manual M9 was published. AWWA C301 and AWWA C304 were termed as manufacturing standard and design standard of PCCP respectively. In 1999, AWWA C301 was revised. In 2006, revised drafts were prepared for AWWA C301 and Manual M9. In 2007, revised AWWA C301 and AWWA C304 were published, which is latest revision in the PCCP standard. The major changes in the design of PCCP includes maximum diameter of the PCCP, strength of concrete, thickness of steel cylinder, prestressing wires, mortar coating. Consequently, the performance of PCCP has been improving over the time in its sixty year history.

According to ACPPA, ninety percent of the largest water utilities in the USA use PCCP. According to Prosser (1996), compare to other pipe materials PCCP has lowest water main break rate per 62 mile. The main advantages of PCCP are resistant to physical damage, economic installation, and corrosion resistance. Although it has some advantages, careful installation is required to avoid cracking. In addition to this, broken pre-stressing wires due to corrosion, poor bedding, and excessive external loading are main causes of PCCP failure.

1.3 PCCP Elements and Material Properties

According to AWWA M9 manual, PCCP is generally constructed of two types; a steel cylinder lined with a concrete core and a steel cylinder embedded in a concrete core. The former type is called PCCP-LCP and the latter type is called PCCP-ECP, which are shown in Figures 1.1(a) and (b) respectively.

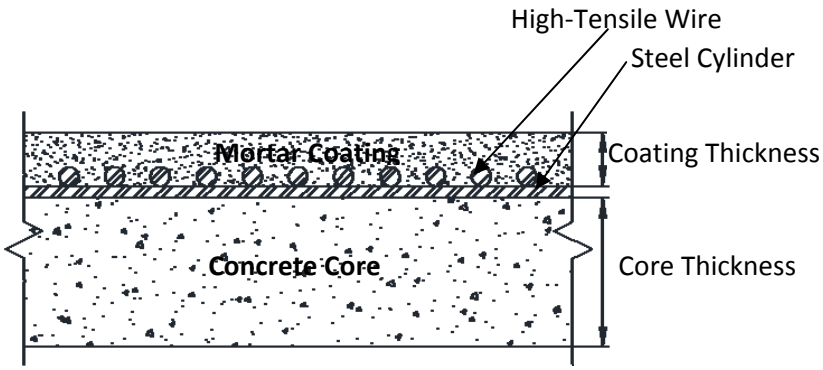

Figure1.1(a) Longitudinal section of wall of PCCP-LCP

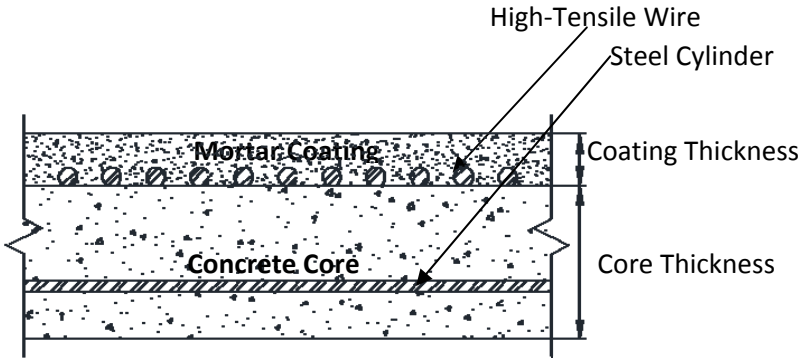

Figure1.1(b) Longitudinal section of wall of PCCP-ECP

PCCP is a composite pipe that consists of concrete and steel, which has layers of concrete core, steel cylinder, pre-stressing wire, and mortar coating as shown in Figure 1.1(a) and 1.1(b). Since the research is related to PCCP-ECP, only PCCP-ECP is explained in detail in this paper.

1.3.1 Concrete Core

This is the main structural element of PCCP-ECP. It is generally casted by two methods: centrifugal method; vertical cast method. Concrete casted by former method is called spun concrete, and concrete casted by latter method is called cast concrete. According to AWWA C301, the minimum 28 days strength of concrete core required is 6000 psi and 4500 psi for spun and cast concrete respectively. In addition, the minimum strength of concrete core required at the wrapping is 4000 psi and 3000 psi respectively for spun and cast concrete. AWWA C301 also impose the condition of initial stress not to exceed the fifty five percent of its strength at wrapping. The material property is shown in Figure 1.2.

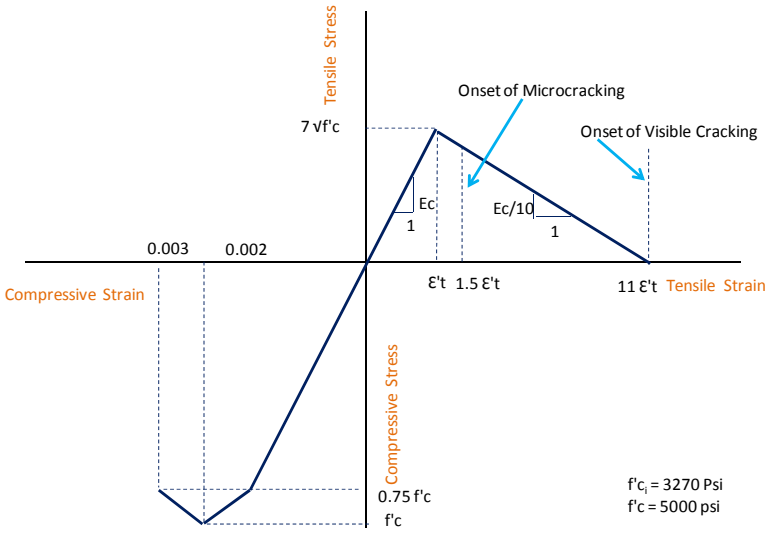

Figure 1.2 Material properties of concrete core (AWWA C304)

1.3.2 Steel Cylinder

Although steel cylinder is not considered as a structural member in PCCP-ECP, it acts as water barrier. According to AWWA C301, the minimum required thickness of steel cylinder is 0.0598 inch. Its design yield strength and modulus of elasticity are 33,000 psi and 30,000,000 psi respectively. The material property is given in Figure 1.3.

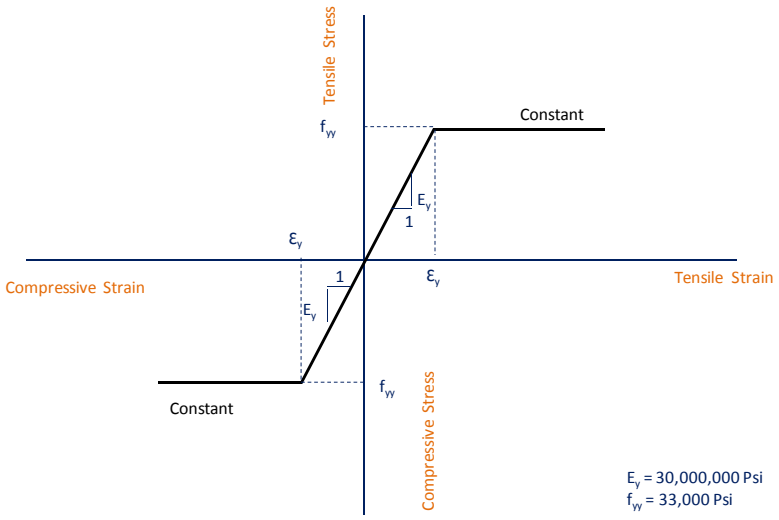

Figure 1.3 Material properties of steel cylinder (AWWA C304)

1.3.3 Prestressing Wire

High tensile pre-stressing wire is wrapped around the concrete core inducing the compression in concrete core. Since concrete is good in compression and weak in tension, prestressing force increases the efficiency of concrete. However, excessive prestressing could cause failure at wrapping stage. Also, exceeding the yield stress of prestressing of wire makes it futile. Therefore, AWWA C304 has imposed condition of prestressing stress in wire not exceeding the seventy five percent of ultimate strength and eighty eight percent of yield strength. The material property is given in Figure 1.4.

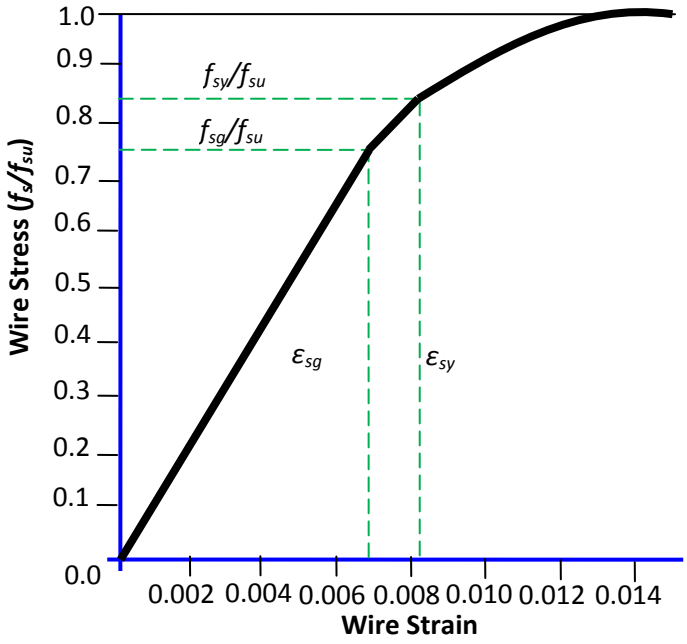

Figure 1.4 Material properties of prestressing wire (AWWA C304)

1.3.4 Mortar Coating

This is the outermost layer of PCCP-ECP, which is made of rich cement sand mortar. It increases alkalinity of PCCP-ECP thus protecting it from aggressive environment, especially from corrosion of pre-stressing wire. According to AWWA C301, the minimum required thickness and 28 days strength of mortar coating are 0.75 inch and 5500 psi respectively. The material property is given in Figure 1.5.

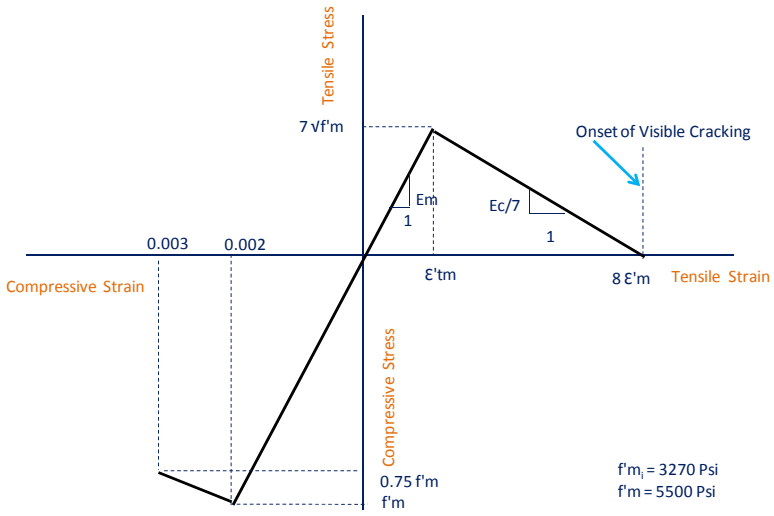

Figure 1.5 Material properties of Mortar coating (AWWA C304)

1.4 Production Method

The method of production of PCCP is categorized on the basis of casting of concrete core. The concrete core can be placed by centrifugal-casting method, radial-compaction method, and vertical-casting method. The concrete core placed by centrifugal-casting method and vertical-casting method are termed as spun concrete and cast concrete respectively. According to AWWA C304, the concrete core casted by radial-compaction method has strength, shrinkage, and creep properties equivalent to that of centrifugal-casting method, which allows it to be termed as spun concrete.

According to AWWA C301, the first step in manufacturing of PCCP-LCP is to fabricate and hydrostatically test the steel cylinder with joint rings attached. The cylinder is then lined with concrete to form the core, which can be placed by any of the method as explained above. The concrete core is cured to allow is to attain certain strength, at least minimum required defined by AWWA C301, and prestressing wire is helically wrapped around the core directly on the steel cylinder. The gross wrapping stress and spacing of prestressing wire is predetermined by considering the residual compression in the core to meet the design requirement for assumed

wire class and size. Finally, the wrapped core is covered with dense premixed mortar coating applied by mechanical impact method, which is done to protect pipe from physical damage and corrosion of prestressing wire.

Similarly, the first step in manufacturing of PCCP-ECP is to construct and test the steel cylinder in the same way that of PCCP-LCP. However, the steel cylinder is encased in concrete by vertical-casting method, and mechanical vibration is applied to constitute the core. The core is cured, and unlike in PCCP-LCP, pre-stressing wire is wrapped around core on outside of concrete core containing the steel cylinder. Finally, the wrapped core is covered with dense premixed mortar coating like in PCCP-LCP.

1.5 Prestress Loss

Although the concept of prestress was developed in 19th century, the lack of understanding of prestress loss delayed its development. Professor G. Magnel is considered among 20th century pioneers, who developed the concept of post tensioning in 1940. There are numerous advantages of prestressing: maintaining gross section properties for improved stiffness; combining concrete with very strength reinforcement; providing active force to close cracks due to overloads. However, it is important to understand prestress losses to utilize advantages of prestressing. The main reasons of prestress losses are as described below.

1.5.1 Elastic shortening

Concrete is also an elastic material, as soon as the stress is applied to the section, the section shortens, thus reducing the extended length of the prestressing wire and hence the stress in it. This loss is the function of elastic modulus of concrete, elastic modulus of wire, and the stress at wrapping.

1.5.2 Shrinkage and Creep

Shrinkage is the phenomenon of reduction in volume of concrete due to hardening of concrete. This is defined as inelastic deformation due to sustained loading on concrete in compression. Shrinkage and creep are function of time, relative humidity, volume to surface ratio, age at loading, curing duration, concrete composition, and method of placement.

1.5.3 Relaxation of wire

This is defined as loss in stress in wire after a period of time. This is the property of wire and it is dependent on initial stress and time period of stress.

1.6 Pipe Installation

According to AWWA M9 manual, the bedding of pipe significantly affects the load carrying capacity of the pipe, which also governs the design of pipe. It is common practice to remove large rocks and debris from backfill placed near the pipe to prevent pipe from external damage. According to AWWA M9 manual, the minimum clearance between the pipe and trench wall should not be less than 9 inch. According to AWWA M9 manual, PCCP-ECP can be installed with different bedding angles as shown in Figure 1.6 (a), (b), (c), (d), and (e). It is common practice to install the PCCP-ECP with higher bedding angle for large diameter pipes.

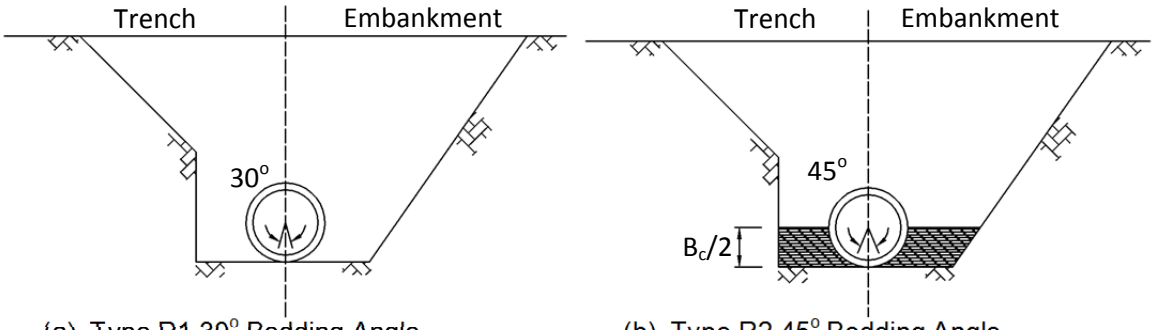

(a) Type R1 30° Bedding Angle

(b) Type R2 45° Bedding Angle

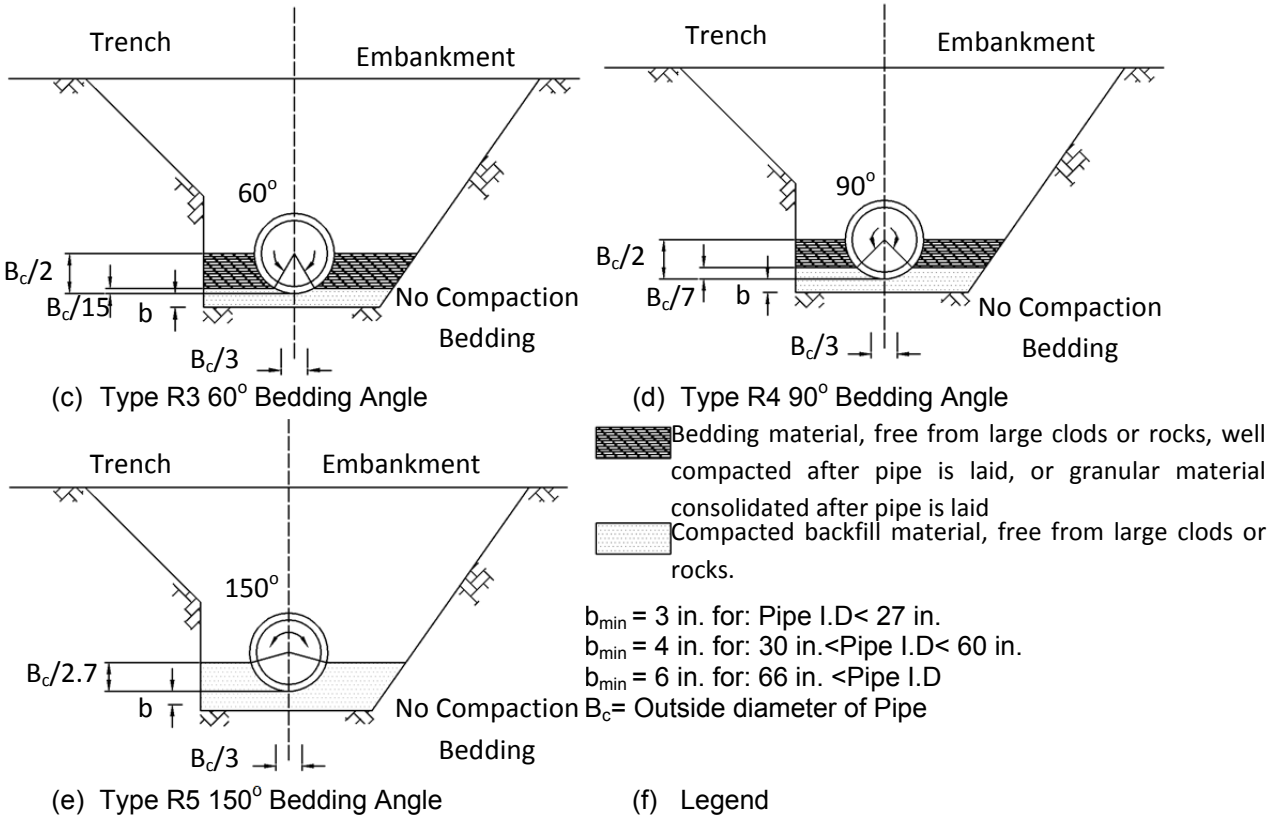

Figure 1.6 Different Installations for rigid pipes (AWWA M9 Manual)

According to Hanson Pipe and Precast, PCCP-ECP is laid on cushion, which is typically 6 inch for pipe having diameter more than 66 inch, of unconsolidated granular material or un-compacted backfill material to achieve uniform support. After the pipe is laid, additional material identical to cushion is placed on the side of pipe up to the desired height based on bedding angle. This total thickness is compacted to obtain 90 % standard Proctor density. After this, backfill material is placed up to spring line in small lift with each lift compacted to obtain 85% of Standard Proctor density.

1.7 Design of PCCP

According to Zarghamee and Dana (1990), pipe industries had been using semi-empirical procedures to design the PCCP until the development of AWWA C301 in 1992, which was unable to consider all the factors that affect the stress in PCCP. They developed the equations to calculate the stress in PCCP considering the effect of shrinkage, creep, and wire relaxation by using step by step integration method. The equations developed by Zarghamee and Dana have been accepted by the current AWWA C304 standard. In addition, shrinkage and creep loss affects the stress in PCCP and relaxation loss, which makes it more complicated phenomenon to calculate stress in PCCP. According to AWWA C304, before the development of this standard, pipe industries had been using two different methods to design PCCP: Method A; Method B.

Method A was based on ninety percent of three-edge bearing test load that causes incipient cracking and theoretical hydrostatic pressure that relieves the calculated residual compression in the concrete core due to pre-stressing. The cubic parabola was used to define allowable combination of three edge bearing load and internal pressure. The three edge bearing load was used to calculate the pipe capacity to bear earth load and transient external load using bedding factors. However, Method B was based on combined net tensile stress in PCCP under static load and internal pressure, which limited the stress to 7.5 $\sqrt{f'_c}$. Both design methods limited the working pressure to decompression pressure for PCCP-ECP and eighty percent of decompression pressure for PCCP-LCP. Decompression pressure is defined as the pressure that just overcomes the compression in the concrete core induced due to pre-stressing.

Although both the methods explained above for PCCP were reliable, new design method, Unified Design Method (UDM), was developed. The purpose of development of this deign method was to avoid the differences between the industries to use design method. UDM incorporates the design criteria defined in both methods A and B. AWWA C304 standard follows the UDM, which has been accepted by all industries in the USA.

1.7.1 AWWA C304 Design Standard

PCCP-ECP is designed and manufactured by following the latest AWWA C304-07 and AWWA C301-07 standards respectively. This design considers the following limit states.

1.7.1.1 Serviceability at full pipe circumference

The purpose of this limit state is to preclude the concrete core from decompression, and to preclude the cracking of the mortar coating.

1.7.1.2 Serviceability at invert/ crown

The purpose of this limit state is to preclude onset of micro cracking and visible cracking of concrete core.

1.7.1.3 Serviceability at spring line

The purpose of this limit state is to preclude micro cracking and visible cracking of mortar coating, and to preclude onset of concrete core micro cracking and core compression.

1.7.1.4 Elastic limit at invert/ crown

The purpose of this limit state is to preclude the stress in steel cylinder exceeding the yield stress.

1.7.1.5 Elastic limit at spring line

The purpose of this limit state is to preclude stress in pre-stressing wire from exceeding gross wrapping stress, and to preclude the stress in concrete core from exceeding seventy-five percent of its design strength.

1.7.1.6 Strength at spring line

The purpose of this limit state is to preclude the stress in pre-stressing wire from exceeding the yield stress.

1.7.1.7 Burst pressure

The purpose of this limit state is to preclude the pipe from burst failure.

1.7.2 AWWA C304 Design Basis

It is worth noting that design of PCCP-ECP also depends on installation type. According to Concrete Pipe Handbook, although Marston developed formulas for calculating earth loads on buried pipe, the importance of bedding was first explained by Spangler in 1933. In 1950, Olander developed coefficients for moment, shear, and thrust for several bedding angle installation, which are based on linear elastic analysis as explained by Concrete Pipe Handbook. Since soil pipe interaction is complex phenomenon, the relatively simplified theories developed by Marston, Spangler, and Olander does not consider all conditions that influence the soil pipe system. Moreover, PCCP-ECP is a composite material with complicated stress phenomenon due to prestress. The design method in AWWA C304 has considered the moment, shear, and thrust coefficients developed by Olander. Moreover, the formulas adopted by AWWA to calculate stress at different stage, from initial to final prestress, are based on step by step integration method, and it does not consider the non-linear behavior due to contact and interaction of pipe components.

1.8 Analysis of PCCP

It is practically infeasible to conduct experimental analysis for each different PCCP-ECP since all PCCP-ECP is custom designed. A study on non-linear finite element analysis of PCCP with broken wires was conducted by Zarghamee et al. (2004). They had modeled the Pipe as composite shell and prestress was applied in radial direction, which does not consider the interaction between prestressing wire and concrete core. Study conducted by Diab and Bonierbale (2001), Lotfi et al. (2005), and Gomez (2004) also considers similar concept of prestress modeling. These proposed methods also fail to consider the relation between stress state prestressing wire and prestress force in concrete core. In addition, the proposed method does not consider the stiffness of prestressing wire and effect of tangential stress due to

prestress. Moreover, it does not consider the effect of shrinkage, creep, and relaxation on material behavior of PCCP-ECP components.

Therefore, it is necessary to develop non-linear three dimensional finite element model of PCCP-ECP by incorporating the non-linear behavior of all its components to simulate the real pipe behavior, which considers the simultaneous effect of shrinkage, creep, and relaxation loss as well as interaction between layers, and manufacturing process.

CHAPTER 2

EXPERIMENTAL EVALUATION

The three-edge bearing tests on two PCCP-ECPs were conducted at Hanson Pipe and Precast, which is located at Grand Prairie, Texas, USA, which is shown in Figure 2.1. The PCCP-ECPs were loaded until four percent vertical deflection. The loads and corresponding vertical and horizontal were recorded. In addition, loads and corresponding crack widths were measured on the PCCP-ECP. Finally, the loads versus displacement graph are plotted and, load corresponding to 0.001 inch crack width is also recorded.

Figure 2.1 PCCP-ECP test site

2.1 Three-Edge Bearing

According to Concrete Pipe Handbook, three-edge bearing is common method to determine the structural strength of concrete pipe. Also, according to Zarghamee et al. (1988),

three-edge bearing test is used to evaluate the structural behavior of pipe under external loads. Three edge bearing is conducted according to the procedure defined in ASTM C497-05.

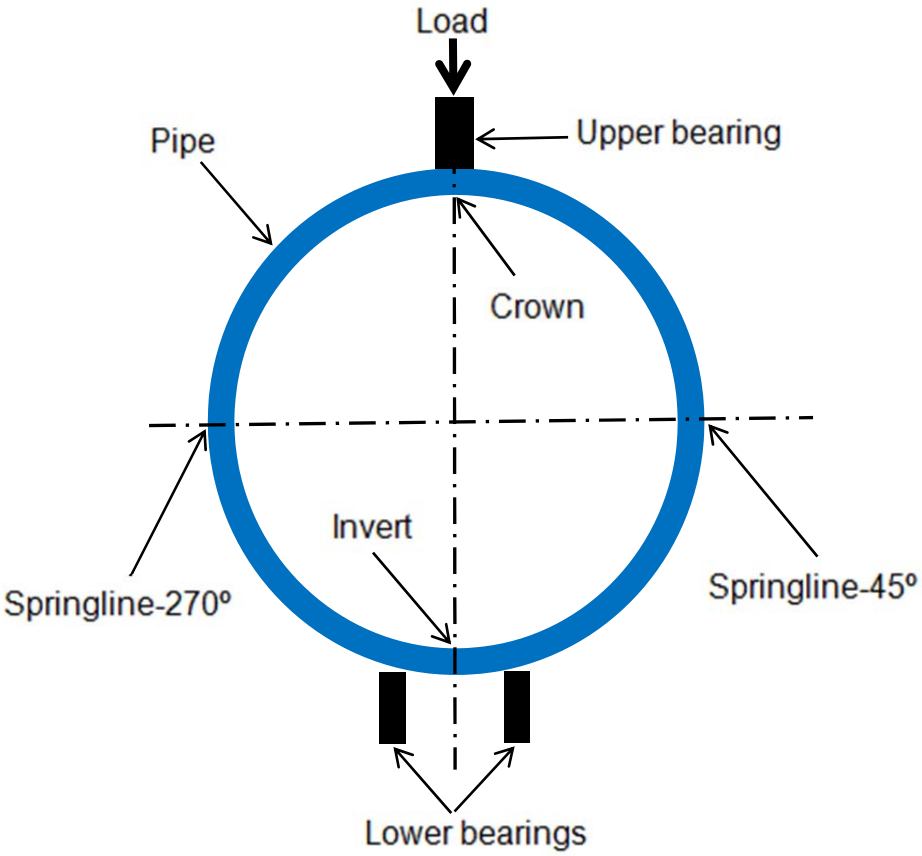

Figure 2.2 Three-Edge Bearing Test Diagram

2.1.1 ASTM C497-05

According to ASTM C497-05, pipe is tested in a machine designed to apply crushing force upon the pipe in a plane through vertical axis extending along the length of the pipe as shown in Figure 2.2. The testing machine should be capable of applying the force without significant deflection of its parts to avoid error in experiment. The testing machine has to be rigid enough to distribute the load evenly to the pipe.

2.1.1.1 Machine requirement

The pipe is supported on two lower bearings and load is applied from top bearing. The length of the bearing strips are usually extended throughout the pipe length although it is optional. According to ASTM C497-05, the lower bearings are made of non-defective wood or hard rubber. If it is wood or rubber, the width of section is two inch minimum, and height should be more than one inch and less than one and half inch. If it is rubber, the durometer hardness should be between forty and sixty. In addition, the distance between two lower bearings should not be more than one inch per one foot of pipe diameter. Also, the top bearing should be made of wood or rubber with same cross section and hardness requirement as explained above for lower bearing.

2.1.1.1 Loading requirement

The pipe is marked at midway between lower two bearings and at top bearing so that pipe can be placed properly to ensure the uniform bearing on each strip. The maximum loading rate for reinforced concrete pipe is 7500 lbf/ linear foot of pipe per minute, and this rate should be used up to seventy five percent of specified design strength as explained by ASTM C497-05. After this, the rate of loading should be one third of the specified design strength of the pipe per minute. This rate of loading should be maintained until the specified design strength is reached; however, this loading rate need not be maintained beyond design strength if ultimate strength is being determined.

2.2 Experiment

The experiment was conducted by following the ASTM C497-05 standard. The experiment was conducted on two ECPs having eighty four inch internal diameter and 5.5 feet length, which is shown in Figure 2.3.

2.2.1 Specimen

The PCCP-ECPs on which the test was conducted were designed according to AWWA/ANSI C304 by assuming following parameters.

2.2.1.1 Geometry

The PCCP-ECP was core casted with following dimensions:

Inside diameter = 84 inch

Outside diameter of steel cylinder = 88 inch

Thickness of core = 5.25 inch

Thickness of mortar coating = 0.942 inch

Thickness of steel cylinder = 0.0598 inch

Diameter of pre-stressing wire = 0.192 inch

Area of pre-stressing wire per foot length of pipe = 0.712 square inch

Outside diameter = 96.38 inch

Figure 2.3 PCCP-ECP on three-edge bearing testing machine

2.2.1.2 Material properties

Compressive Strength of concrete core at maturity = 5000 psi

Tensile strength of concrete core at maturity = 495 psi

Compressive Strength of concrete core at wrapping = 3270 psi

Compressive Strength of mortar coating at maturity = 5500 psi

Tensile strength of mortar coating at maturity = 519 psi

Yield strength of steel cylinder = 33,000 psi

Prestressing wire class = ASTM A648 class III

Gross wrapping stress in pre-stressing wire = 189,000 psi

Ultimate strength of pre-stressing wire = 252,000 psi

Modular ratio at maturity = 7.501

Modular ratio at wrapping = 8.037

2.2.1.3 Exposure and Installation

Relative humidity = 70 %

Time of pipe from casting to installation = 270 days

Time of pipe from installation to operation = 90 days

Bedding angle = 90 degree Olander

2.2.1.4 Loads

Working Pressure = 150 psi

Transient pressure = 60 psi

Surge pressure = 180 psi

Height of soil above the pipe = 6 ft.

Density of soil = 120 lb/ ft^3

Weight of pipe = 1,839 lb/ ft

Weight of soil on pipe = 6,688 lb/ ft

2.2.2 Instrumentation

The horizontal and vertical deflection of PCCP-ECP during three-edge bearing tests are measured by using Cable extension Displacement Sensor (CDS), which are shown in Figure

2.4(a) and 2.4 (b). The load applied to the pipe through top bearing is measured by using Load cell, which is shown in Figure 2.5.

2.2.2.1 CDS and Load cell

(a) (b)

Figure 2.4 CDS used for measuring deflection of PCCP-ECP (a) Horizontal, (b) Vertical

CDS is a box like device equipped with string. CDS is attached to the one end of the pipe and the string attached to it is connected with opposite side along the diameter of the pipe. When the pipe deflects, string either goes inside or come outside of the box depending upon whether the diameter is decreasing or increasing. For example, if the CDS is attached at invert to measure vertical deflection, and if the load is applied on the top of pipe, then the string goes inside of the pipe. However, the reverse process occurs if the CDS is attached to the spring line to measure horizontal deflection. Also, load cell is device that is connected to the hydraulic load application machine, which reads the load and transfers to the Vishay scanner.

Figure 2.5 Load Cell

2.2.2.2 Vishay Scanner

Vishay scanner, which is shown in Figure 2.6, is a device that has strain smart software. It reads the deflection from CDS and load from load cell, and it plots the data in a user defined form. For example, if user wants to monitor the load versus deflection graph, Vishay scanner automatically plots it. It helps to monitor the experiment as user can watch rate of loading, rate of displacement during the experiment.

Figure 2.6 Vishay scanner

2.2.3 Procedure and experiment

The displacement control experiment was conducted at Hanson Pipe and Precast Plant, which is located at Grand Prairie of Texas, USA. The 84 inch diameter and 5.5 feet long PCCP-ECP was placed on the three edge bearing test machine, which is shown in Figure 2.7, and the procedure was followed as defined by ASTM C497-05.

Figure 2.7 PCCP-ECP placed on testing machine

The lower bearings were kept 7 inch apart. The CDS were attached at the invert and spring line position as shown in Figure 2.8. Then each CDS was attached to opposite end of PCCP-ECP with the means of string attached to it.

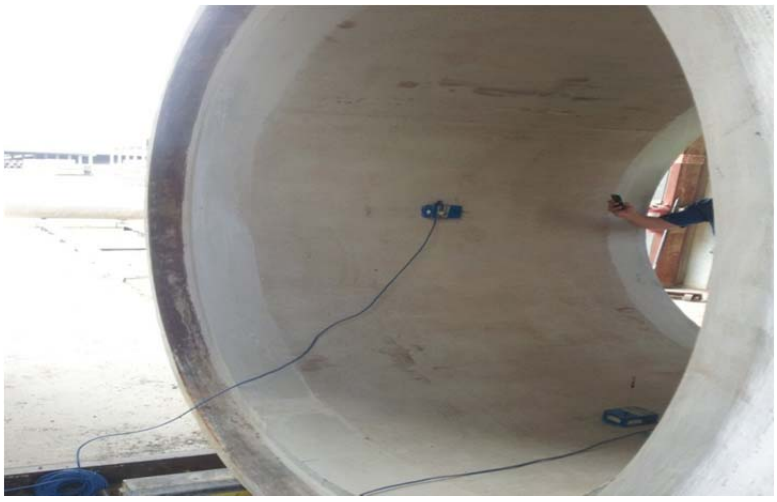

Figure 2.8 CDs attached to the PCCP-ECP

Figure 2.9 Top bearing brought in contact with PCCP-ECP

The top bearing of the machine was brought in contact to the pipe in such a way that no any load was transferred to the PCCP-ECP, which is shown in Figure 2.9. After this, both CDS and load cell were connected to the Vishay Scanner, and the displacements and load were set to zero, which is shown in Figure 2.10 and Figure 2.11.

Figure 2.10 Connection of CDS and load cell to Vishay scanner

Figure 2.11 Setting the load and displacement to zero value

Figure 2.12 Loading the PCCP-ECP through top bearing

The load was then applied at a constant rate as per ASTM C497-05 from the top bearing as shown in Figure 2.12. The loads and corresponding vertical and horizontal displacements were recorded from the beginning to end of the test. The cracks at invert, crown and spring line were measured at different loads, which are explained in detail Table 2.1. The crack widths were measured with crack comparator.

Table 2.1 Observed Crack at different stages of loading

Load (kips)	**Observed**
20	No Cracks
30	No Cracks
40	No Cracks
50	No Cracks; vertical deflection suddenly increased
60	No Cracks
70	No Cracks
75	No Cracks
77	No Cracks
80	No Cracks
86	First crack at invert; 0.001 inch (Figure 2.13)
90	Another 0.001 inch crack near invert (Figure 2.14)

Table 2.1- *Continued*

90	0.001 inch crack at crown (Figure 2.15)
95	0.01 inch crack at invert (Figure 2.16)
97	separation of mortar coating from concrete core started (Figure 2.17)
100	0.016 inch crack at crown (Figure 2.18)
100	0.02 inch crack at invert (Figure 2.19)
100	hair line crack at spring line
110	0.06 inch crack at crown (Figure 2.20)
110	0.05 inch crack at invert (Figure 2.20)
110	0.016 inch crack at spring line (Figure 2.21)

The pictures of different events during experiment are given below.

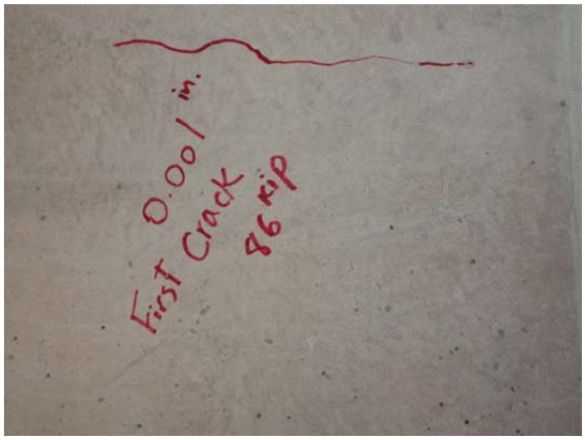

Figure 2.13 First crack (0.001 inch) at invert

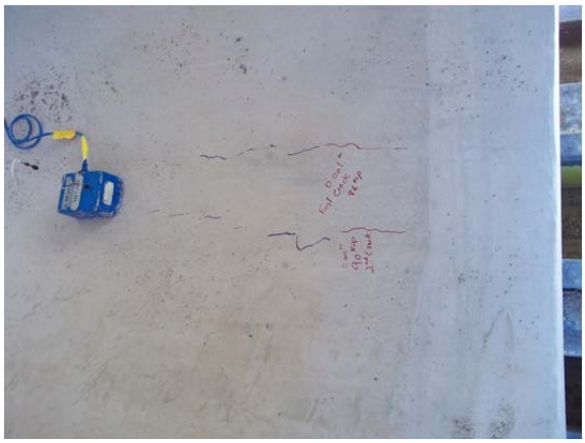

Figure 2.14 Second crack at invert

Figure 2.15 0.001 inch crack at crown

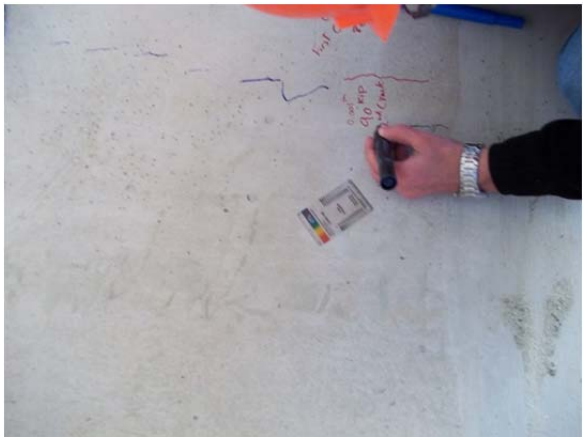

Figure 2.16 0.01 inch crack at invert

Figure 2.17 Delamination of mortar coating from core

Figure 2.18 0.016 inch crack at crown

Figure 2.19 0.02 inch crack at invert

Figure 2.20 Cracks at invert and crown

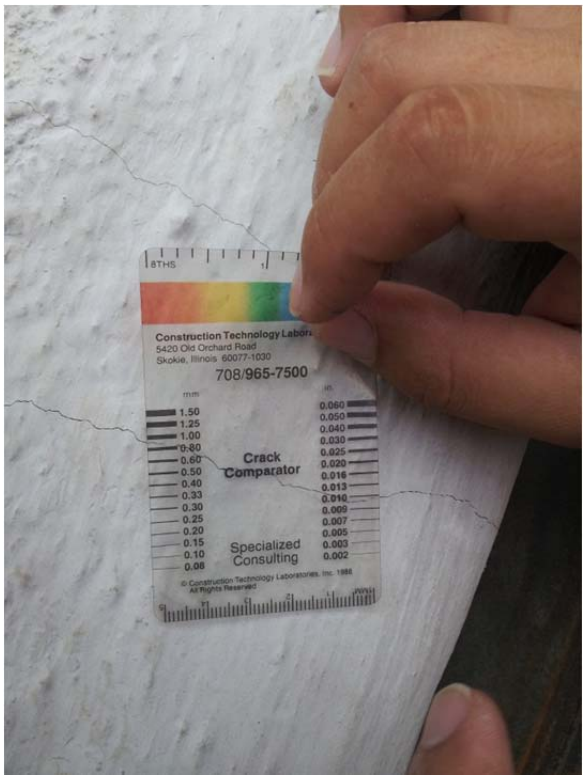

Figure 2.21 Crack at spring line

2.2.4 Test Result

The load is plotted along y axis and percentage vertical deflection is plotted along x-axis, which is shown in Figure 2.23(a) and (b). Figure 2.23(a) is result obtained from first experiment, and Figure 2.23(b) is result obtained from experiment 2. It should be noted that the load-displacement graph, which is shown in Figure 2.23(a) and (b), are plotted for full length of pipe specimen, which was 5.5 feet.

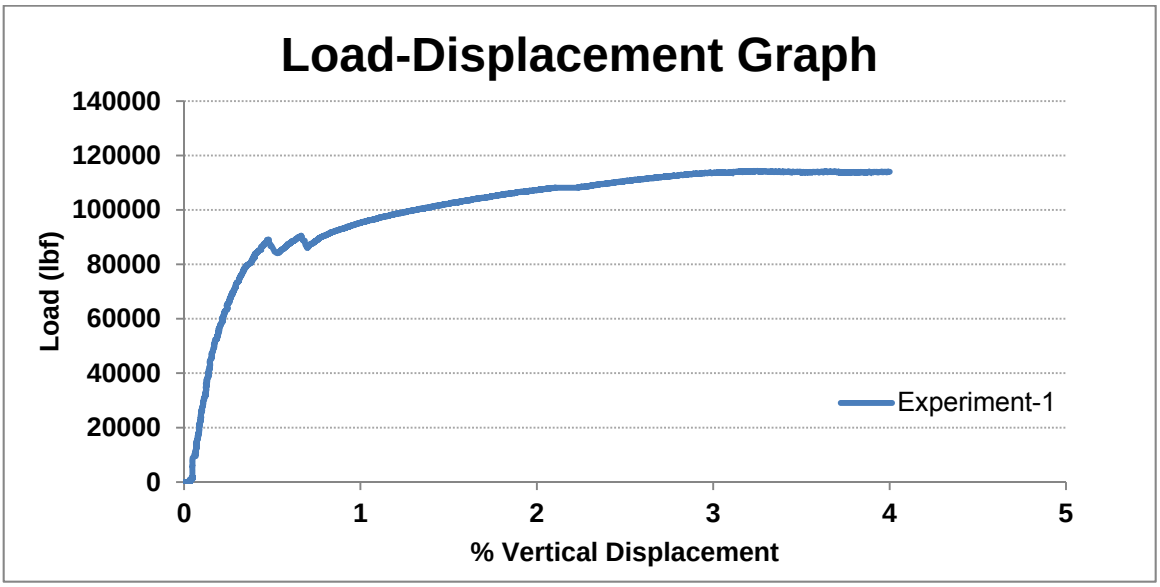

(a)

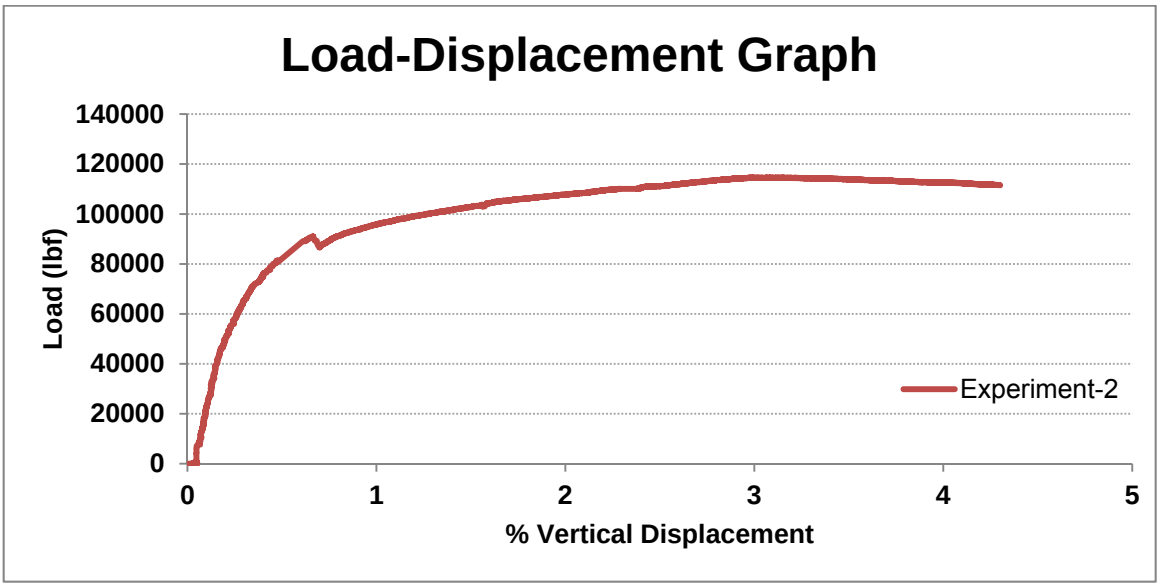

(b)

Figure 2.22 (a) Experiment 1 result, (b) Experiment 2 result

CHAPTER-3

FINITE ELEMENT MODEL

3.1 Introduction

The three dimensional finite element analysis of PCCP-ECP is modeled in Abaqus, a Finite Element Modeling (FEM) software. The analysis is performed by considering the practical possibilities. The contact between different layers of PCCP-ECP, concrete core, steel cylinder, prestressing wire, and mortar coating, are carefully modeled. The elements of the model are eight nodded. The mesh sizes are defined on the basis of possible distortion and size of elements.

Also, the non-linearities due to material properties, contact, and geometry are considered. The PCCP-ECP is modeled by considering the manufacturing steps, and all the stresses at different stages are considered. Furthermore, the three-edge bearing test is performed by finite element analysis to compare the PCCP-ECP behavior with real PCCP-ECP. The modeled PCCP-ECP is shown in Figure 3.1.

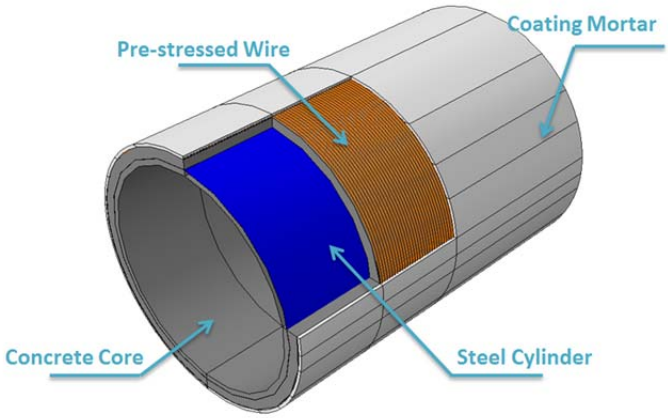

Figure 3.1 Modeled PCCP-ECP

3.2 FINITE ELEMENT MODELING

At present, the finite element method is the most powerful numerical technique for performing complex structural analysis, which can be used for both linear and non-linear analysis. Non-linear analysis includes material yielding, crack formation, buckling and post-buckling, material contact, and friction, which allows to simulate the real structural system behavior to a great extent of accuracy. Moreover, it can be used for both static and dynamic analyses.

3.2.1 Preliminaries of Material Modeling

A material model is a set of mathematical equations that describes the relationship between stress and strain. Material models are often expressed in a form in which infinitesimal increments of stress or stress rates are related to infinitesimal increments of strain or strain rates. All material models implemented in this study are based on a relationship between the stress rates, σ ' and the strain rates, ε '.Stress is a tensor which can be represented by a matrix in Cartesian coordinates:

$$\sigma = \begin{bmatrix} \sigma_{xx} & \sigma_{xy} & \sigma_{xz} \\ \sigma_{yx} & \sigma_{yy} & \sigma_{yz} \\ \sigma_{zx} & \sigma_{zy} & \sigma_{zz} \end{bmatrix}$$

In the standard deformation theory, the stress tensor is symmetric such that $\sigma_{xy} = \sigma_{yx}, \sigma_{yz} = \sigma_{zy},\ \sigma_{zx} = \sigma_{xz}$. In this situation, stress can be written in notation, which involves only six different components:

$$\sigma = (\sigma_{xx}\ \sigma_{yy}\ \sigma_{zz}\ \sigma_{xy}\ \sigma_{yz}\ \sigma_{zx})^T$$

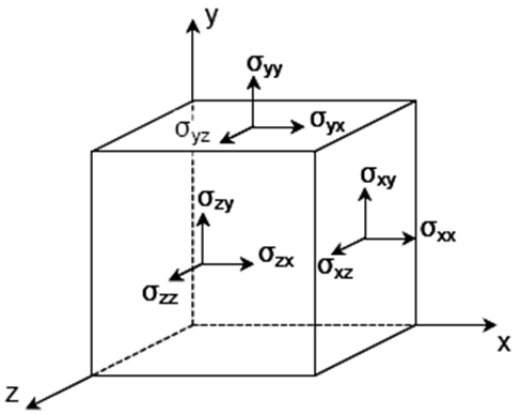

Figure 3.2 General three-dimensional coordinate system for stresses

3.2.2 Element Types

Continuum or solid elements were used to model the various components in PCCP-ECP. Conceptually, continuum elements simply models small blocks of material in a component. All elements were connected together on any of their faces, continuum element, like bricks, were used to create models of nearly shape, subjected to nearly any loading.

The expression full integration refers to the number of gauss points required to integrate the polynomial terms in element's stiffness matrix exactly when the element has regular shape. For hexahedral and quadrilateral elements, a regular shape means that the edges are straight and meet at the right angles and that any edge nodes the midpoint of the edge. Fully integrated, linear elements use two integration points in each direction. The different type of mesh used in the finite element modeling is shown in the figure below.

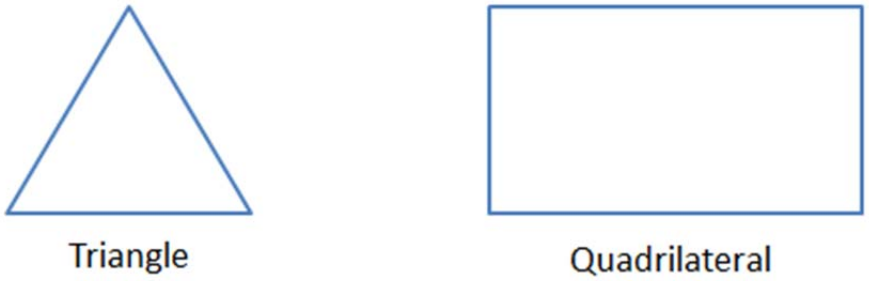

Figure 3.3(a) Two-dimensional mesh types

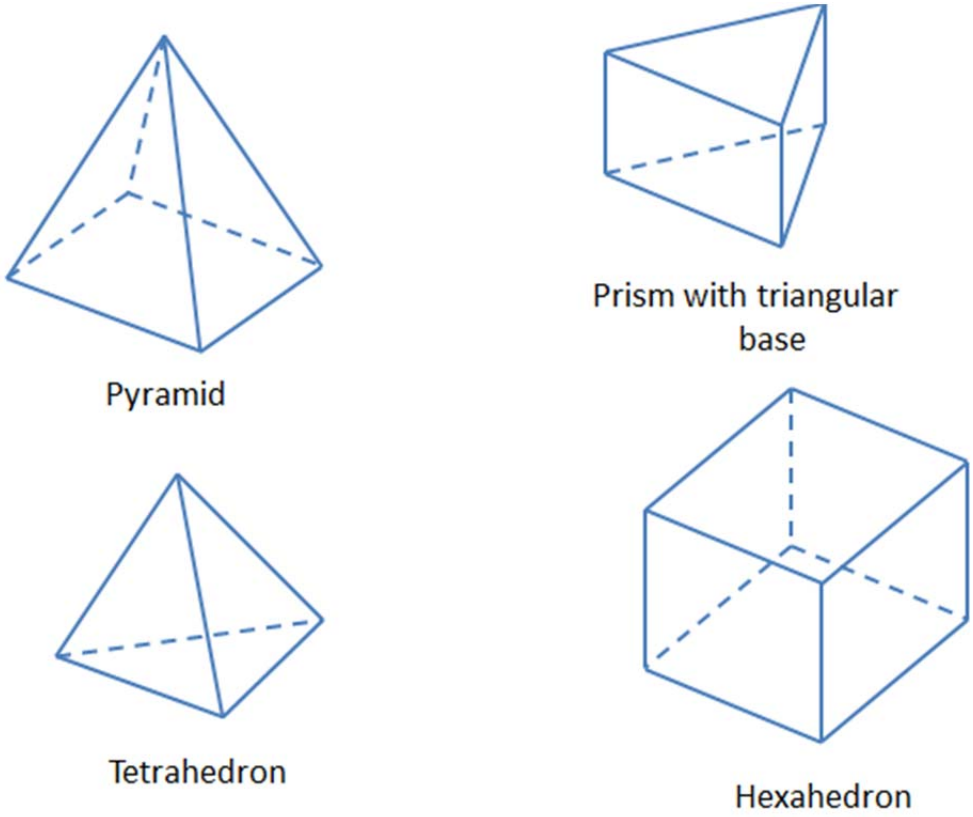

Figure 3.3(b) Three-dimensional mesh types

Only quadrilateral and hexahedron elements can use a reduced-integration scheme; all wedge, tetrahedral, and triangular solid elements use full integration, although they can be used in the same mesh with reduced-integration hexahedral or quadrilateral elements. Reduced-integration elements use one fewer integration point in each direction than the fully integrated elements. Reduced-integration, linear elements have just a single integration point located at the element's centroid. The typical converged meshes are shown in figure 3.4, 3.5, 3.6, 3.7, and 3.8.

Figure 3.4 Converged mesh of concrete core

Figure 3.5 Converged mesh of mortar coating

Figure 3.6 Converged mesh of steel cylinder

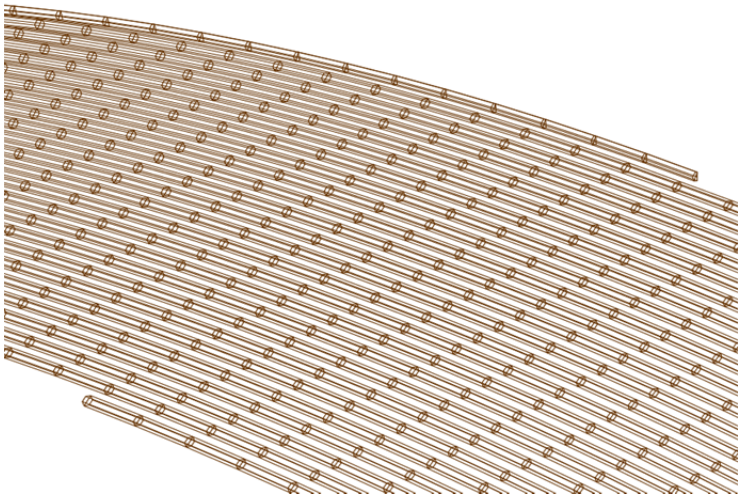

Figure 3.7 Converged mesh of prestressing wire

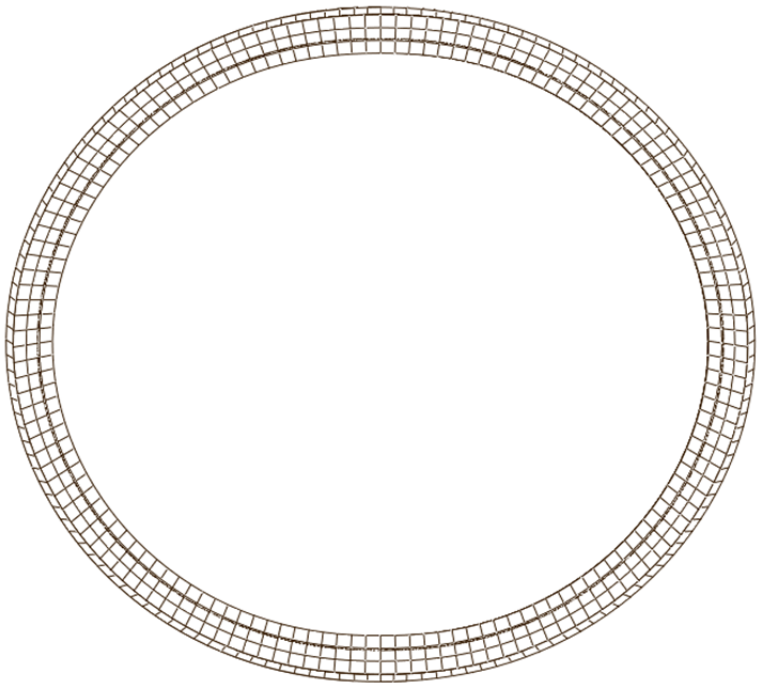

Figure 3.8 Converged mesh of PCCP-ECP

3.2.3 Solid Element Formulation

All solid elements in Abaqus allow for finite strain and rotation in large displacement analysis. For kinematically linear analysis the strain is defined by following equation.

$$\varepsilon = \mathrm{sym}\left(\frac{\partial \mathrm{u}}{\partial \mathrm{X}}\right)$$

In the above equation, X is the spatial position of the point under consideration. If the strains and rotations are small, this measure of strain is useful. If the strains the strains and rotations are not small, two ways of measuring strain are used in the solid elements. If hyperelastic or hyperfoam material definition is assigned to an element, Abaqus internally uses the stretch values calculated directly from the deformation gradient matrix, which compute the material behavior. For other material behavior it is assumed that any elastic strains are small compared to unity, so the appropriate reference configuration for the elasticity is only infinitesimally different from the current configuration and the appropriate stress measure is the Cauchy or true stress. More precisely, the appropriate stress measure should be the Kirchhoff stress defined with respect to the elastic reference configuration, but the assumption that this reference configuration and the current configuration are only infinitesimally different makes the Kirchhoff and Cauchy stress measures almost the same where the differences are on the order of the elastic strains.

3.3 Material Failure Theory

According to Boresi, inelastic behavior can occur under multiaxial stress in the specimen even if none of the individual components of stress exceeds the uniaxial yield stress. Failure of material is generally considered at the initiation of inelastic material behavior through yielding or fracture. According to Mendelson (1983), a complete plasticity theory consists of three components, which are yield criteria, flow rule, and hardening. The material failure behavior is different in ductile material, such as steel, and brittle material, such as concrete.

3.3.1 Steel Failure

It is postulated that yielding is initiated in a multiaxial stress state when stress in material reaches some limiting value, which is function of uniaxial yield stress. Similary, failure by fracture mode can be predicted if appropriate criteria is defined. However, no any yield or fracture criteria has been developed that can accurately establish failure response of material. Nevertheless, the theories exist that reasonably predicts material failure responses. In ductile metals, yield criteria is based on limiting value of shear stress. Two popular theories to determine yield surface are maximum shear stress criteria, which is also called Tresca hexagon, and octahedral shear stress criteria, which is also called Von-mises ellipse. Although former method is simple for calculation, latter method is more popular due its non-discontinuity in failure curve, which is shown in figure 3.9. Therefore, for modeling of steel and prestressing wire, octahedral shear stress criteria is used.

Octahedral shear stress criteria states that yielding begins when the distortional strain energy density at a point equals the distortional strain energy density at yield in uniaxial tension or compression. The total energy can be divided into two parts: volumetric change energy; distortional energy, which is given in equation below. In the equation below, K is bulk modulus and G is shear modulus.

$$U_0 = \frac{(\sigma_1 + \sigma_2 + \sigma_3)^2}{18K} + \frac{(\sigma_1 - \sigma_2)^2 + (\sigma_2 - \sigma_3)^2 + (\sigma_3 - \sigma_1)^2}{12G}$$

$$K = \frac{E}{3(1 - 2\nu)}$$

$$G = \frac{E}{2(1 + \nu)}$$

The distortional energy is given by the equation below.

$$U_0 = \frac{(\sigma_1 - \sigma_2)^2 + (\sigma_2 - \sigma_3)^2 + (\sigma_3 - \sigma_1)^2}{12G} = \frac{1}{2G} J_2$$

$$J_2 = \frac{1}{6}[(\sigma_1 - \sigma_2)^2 + (\sigma_2 - \sigma_3)^2 + (\sigma_3 - \sigma_1)^2]$$

$$J_2 = I_2 + \frac{1}{3} I_1^2$$

The yield function is given by the equation below.

$$f = \frac{1}{6}[(\sigma_1 - \sigma_2)^2 + (\sigma_2 - \sigma_3)^2 + (\sigma_3 - \sigma_1)^2] - \frac{1}{3} Y^2$$

$$\tau_A = \frac{Y}{\sqrt{3}}$$

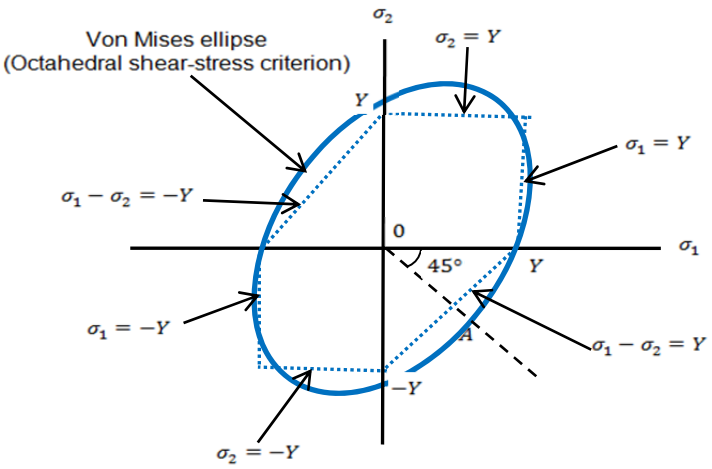

Figure 3.9 Von Mises yield surface

3.3.2 Concrete Failure

Concrete is widely known material that is used in structures. It is also well known fact that concrete is very good in compression and weak in tension. It is often ignored the tensile strength of concrete in analysis of reinforced concrete beam assuming that compression part never undergoes tension. However, there are situations when concrete undergoes tension and development of crack plays significant role. This type of problem is solved by considering plasticity theory in compression zone and analyzing tensile zone, where at least one principal stress is tensile, by fracture mechanics theory such as smeared crack modeling (Rashid, 1968), the fictitious crack model (Hillerborg et al., 1976), linear elastic fracture mechanics (Bezant and Cedolin, 1980), and crack band theory (Bazant and Oh, 1983).

According to Onate et al. (1986), the above mentioned modeling techniques to deal with tension zones in concrete have several drawbacks, such as unable to use of a quite arbitrary shear retention factor to ensure some shear resistance along the crack and unable to attain equilibrium at cracking point when multiple cracks are expected. In addition, according to De Borst (1987), in above mentioned modeling techniques it is difficult to define the stress path following the opening and closing of cracks under cyclic loading condition and it makes difficult to analyze the combined effect of cracking and plasticity. However, according to Lubliner et al. (1989), the above mentioned limitations can be overcome by defining the single constitutive model that governs the non-linear behavior of concrete including failure in both compression and tension, which is called concrete plasticity damage theory. Lubliner et al. proposed the theory based on an internal variable formulation of plasticity theory and new yield criteria, which matched the experimental data for concrete.

Lubliner et al. (1989) replaced the hardening variable of classical plasticity theory by plastic damage variable. This yield surface adopted by these authors is defined by the equation below and figure 3.10.

$$F(\sigma) = \frac{1}{1-\alpha}[\sqrt{3J_2} + \alpha I_1 + \beta < \sigma_{max} > -\gamma < -\sigma_{max} >]$$

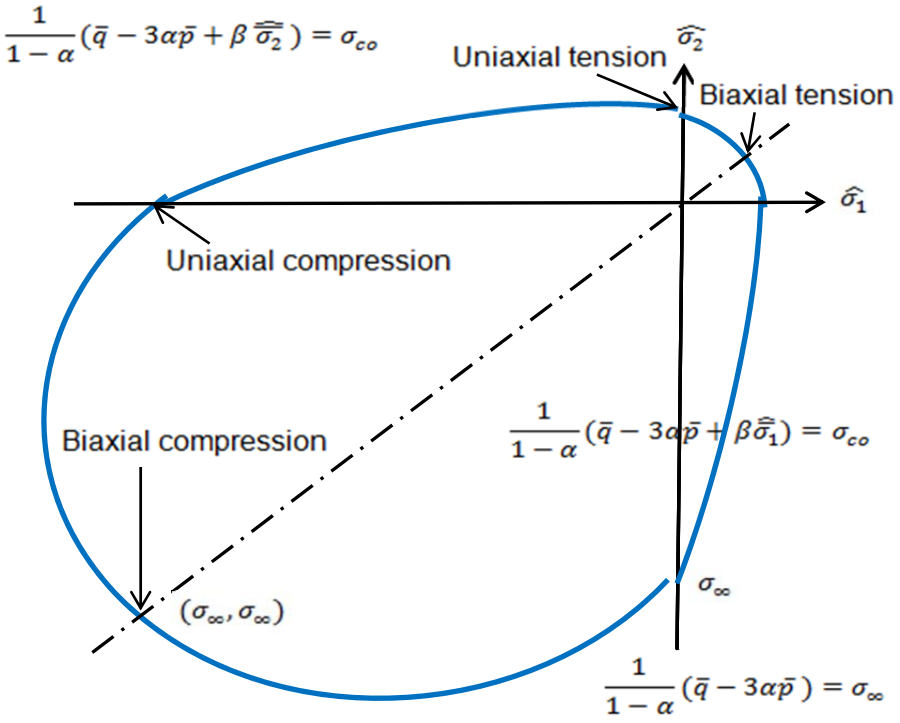

Figure 3.10 Concrete yield surface in plane stress

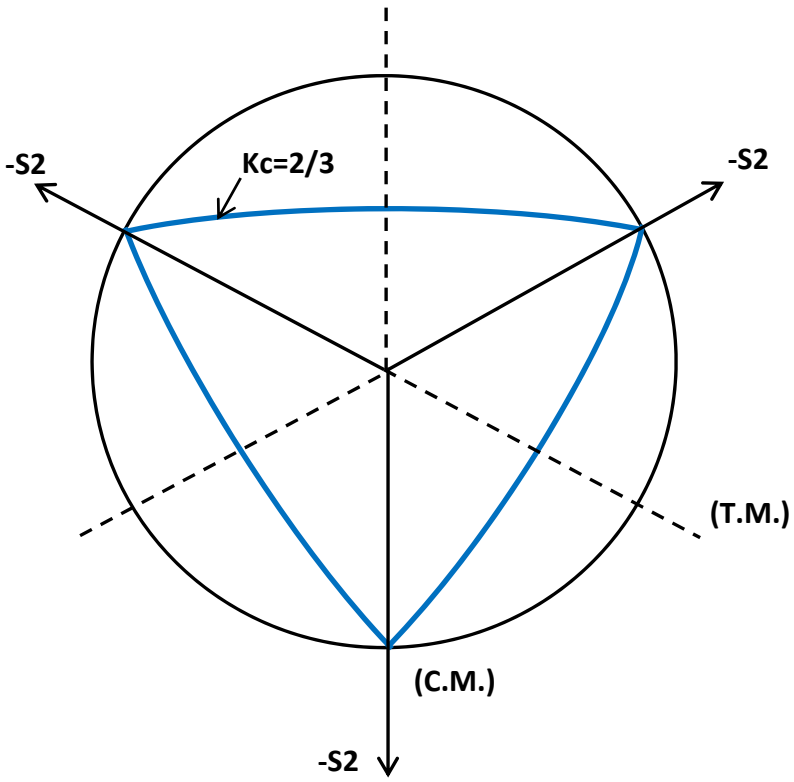

Figure 3.11 Yield surfaces in deviatoric plane corresponding to different value of Kc

In the above equation α, β, and γ are dimensionless constants. In biaxial compression, $\sigma_{max} = 0$. The value of α lies between 0.08 and 0.12 per observed in experiments. The parameter γ is valid only for triaxial compression or the state of being $\sigma_{max} < 0$. In the figure 3.11, (T.M.) and (C.M.) represents tensile and compression meridian respectively.

For tensile meridian ($\sigma_1 > \sigma_2 = \sigma_3$),

$$\sigma_{max} = \frac{1}{3}(I_1 + 2\sqrt{3J_2}\,)$$

For triaxial compression,

$$(2\gamma + 3)\sqrt{3J_2} + (\gamma + 3\alpha)I_1 = (1 - \alpha)f_c$$

For compressive meridian ($\sigma_1 = \sigma_2 > \sigma_3$),

$$\sigma_{max} = \frac{1}{3}(I_1 + \sqrt{3J_2}\,)$$

For triaxial compression,

$$(\gamma + 3)\sqrt{3J_2} + (\gamma + 3\alpha)I_1 = (1 - \alpha)f_c$$

Where f_c is the critical stress in uniaxial compression.

The multiaxial behavior of concrete with degradation behavior states that bulk modulus depends primarily on the volume strain, and shear modulus on the octahedral shear strain as reported by Cedolin et al. (1977) and Andanaes et al. (1977). The bulk and shear moduli are given by the equations below.

$$K = (1 - d_1)K_0$$

$$G = (1 - d_2)G_0$$

The 6 x 6 stiffness matrix of an isotropic solid is given below.

$$D = KII^T + GU\ dev$$

In the above equation,

$$I = (1,1,1,0,0,0)$$

$$dev = I - \frac{1}{3}II^T$$

$$U = \begin{bmatrix} 2 & 0 & 0 & 0 & 0 & 0 \\ 0 & 2 & 0 & 0 & 0 & 0 \\ 0 & 0 & 2 & 0 & 0 & 0 \\ 0 & 0 & 0 & 1 & 0 & 0 \\ 0 & 0 & 0 & 0 & 1 & 0 \\ 0 & 0 & 0 & 0 & 0 & 1 \end{bmatrix}$$

3.4 Plane-Strain Approximation

In real engineering components, stresses are three dimensional tensors. However, when the dimension of one side is much greater than other two sides, the strain associated with longer side and shear strains along longer side are small compared to cross sectional strains. Plain strain approximation is commonly used in the analysis of pipe; however, PCCP is helically wrapped pipe around the core, which makes prestressing wire out of plane at any cross section, which is shown in Figure 3.12(a) and 3.12(b). As a result, two dimensional analysis of PCCP cannot be accurate. Therefore, three dimensional analysis is done in this research.

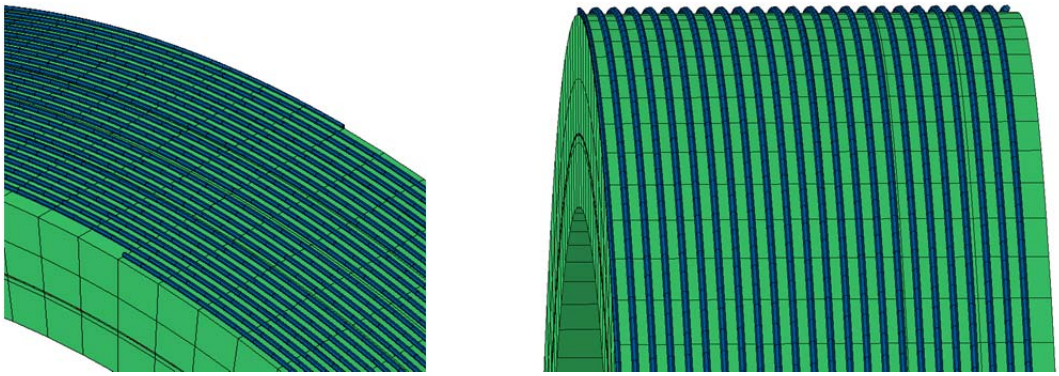

(a) (b)

Figure 3.12 Prestressing wire wrapped on concrete core

3.5 Modeling of PCCP-ECP

The finite element model of PCCP-ECP is created with the full diameter. Although the pipe can be modeled with considering symmetric half part, considering diameter as a divider, full diameter is modeled to simulate the cracks and three edge bearing test. The material properties considered for the analysis are given below, which considers the non-linear behavior of PCCP-ECP components. Although the experiment was done on 5.5 feet long PCCP-ECP, only 1 foot length is created for finite element analysis due to its high computational time.

3.5.1Components and Material Modeling

The 84 inch diameter PCCP-ECP is modeled by considering the manufacturing process, and all components are modeled carefully.

3.5.1.1 Concrete core

Concrete core is modeled as solid three dimensional axis-symmetric element as shown in Figure 3.13. The inside diameter of the core is 84 inch and outside diameter is 89.25 inch. The material properties considered for the core us shown in Figure 3.14.

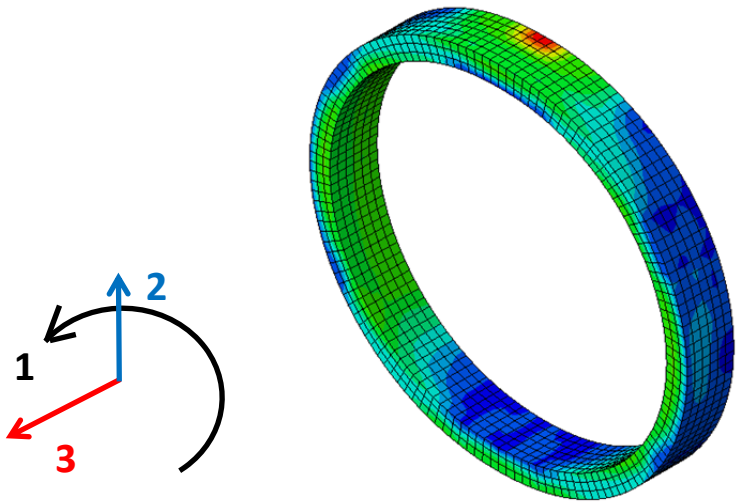

Figure 3.13 Modeled concrete core

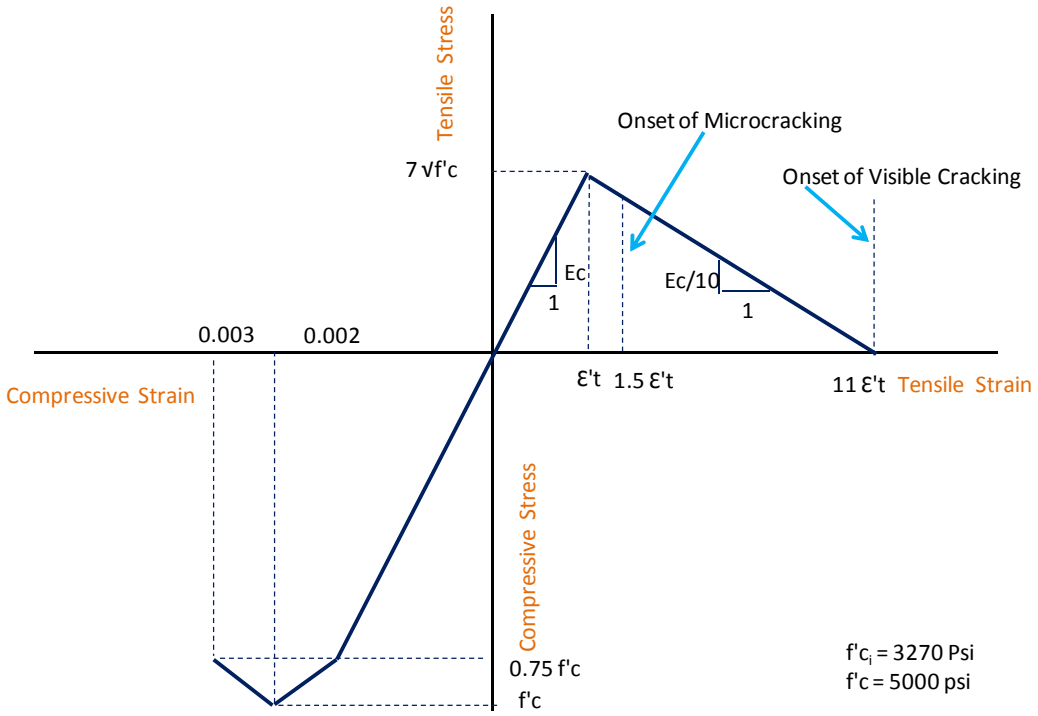

Figure 3.14 Material properties of concrete core

The concrete core is considered as host material and steel cylinder is considered as embedded material. This feature allows the host material, concrete core in this case, to control the distortion of embedded material, steel cylinder in this case.

In fact, the embedded material becomes part of host region and shares the common mesh. In reality, the steel cylinder is sandwiched in concrete core during casting and is restrained in all direction relative to concrete core. Therefore, the assumption in finite element is reasonable. The concrete core is modeled by considering concrete plasticity damage.

3.5.1.2 Steel Cylinder

The steel cylinder is modeled as solid element although the thickness is only 0.0598 inch, which is shown in Figure 3.15.

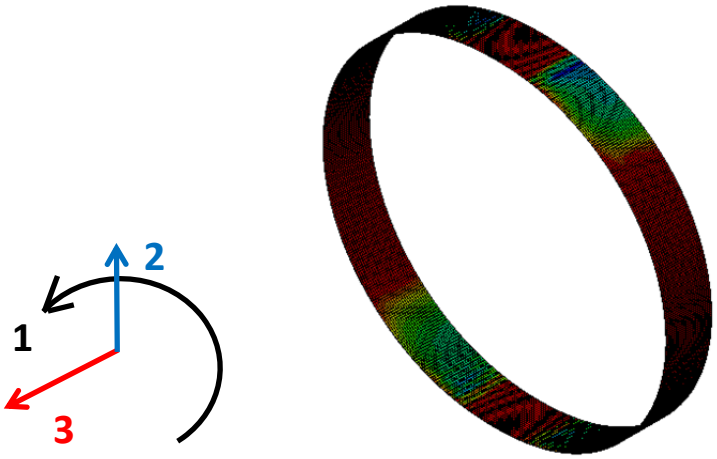

Figure 3.15 Modeled steel cylinder

This serves as water barrier. Although the steel cylinder is not considered as structural element in PCCP-ECP, it plays role in interaction with concrete core during shrinkage, creep, and prestressing. The material property of steel cylinder is defined as elastic –perfectly plastic material, which is shown in Figure 3.16.

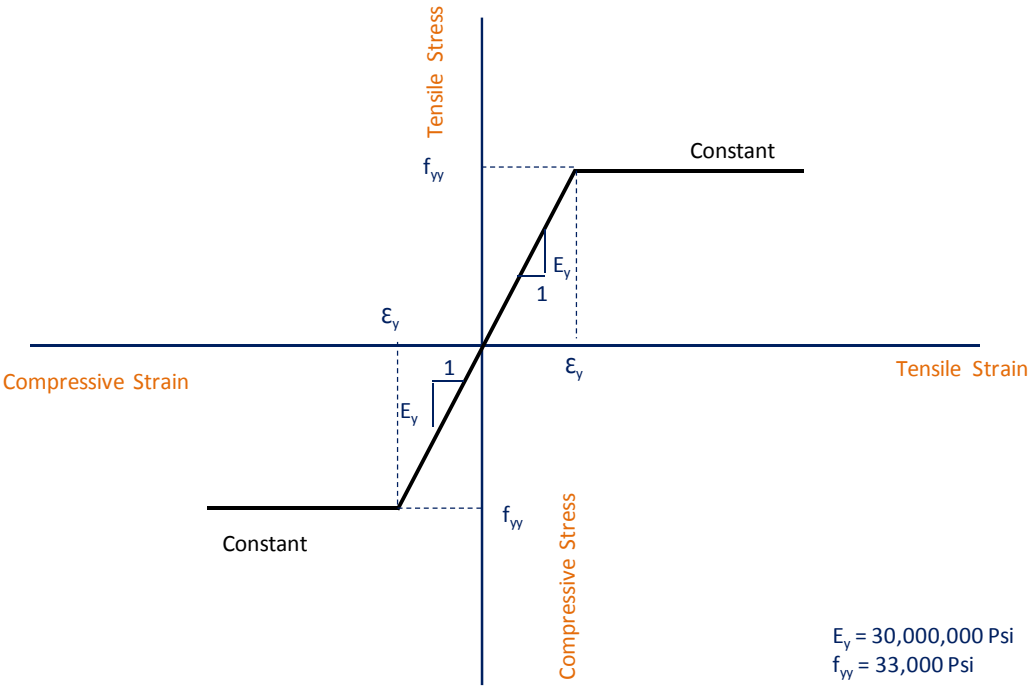

Figure 3.16: Material properties of steel cylinder

3.5.1.3 Prestressing wire

The prestressing wire is defined as solid helical bar of diameter 0.192 inch. The spacing is defined in such a way that total cross sectional area is 0.712 square inch per foot of pipe. Figure 3.17(a). 3.17(b), and 3.17 (c) shows the modeled pre-stressing wire.

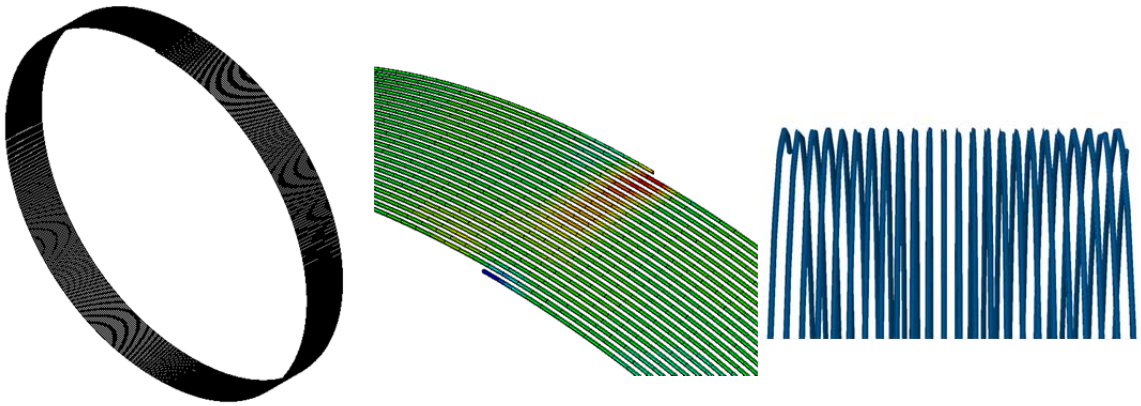

(a) (b) (c)

Figure 3.17 Modeled prestressing wire :(a) view 1, (b) view 2, (c) view 3

The material property of prestressing wire is considered as shown in Figure 3.18.

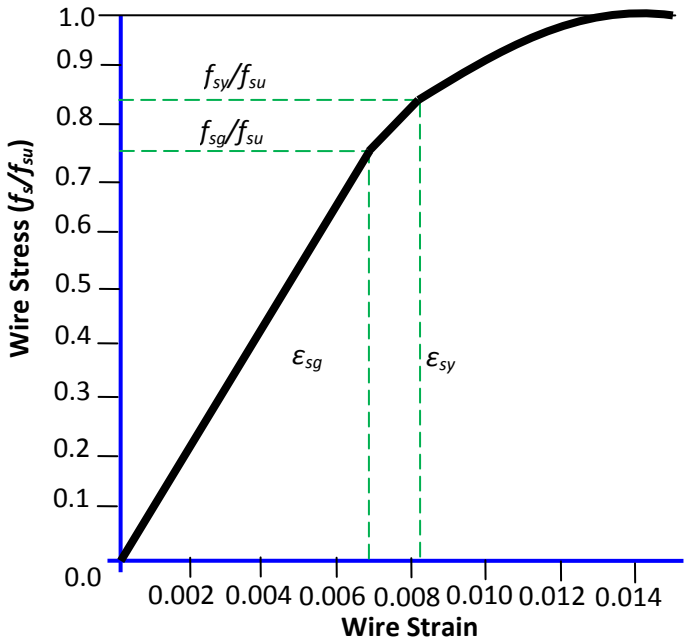

Figure 3.18 Material properties of prestressing wire

3.5.1.4 Mortar coating

Mortar coating is modeled as solid axisymmetric element. The outside diameter is considered as 88 inch and inside diameter as 87.058 inch, which is shown in Figure 3.19. The material properties are defined as shown in Figure 3.20.

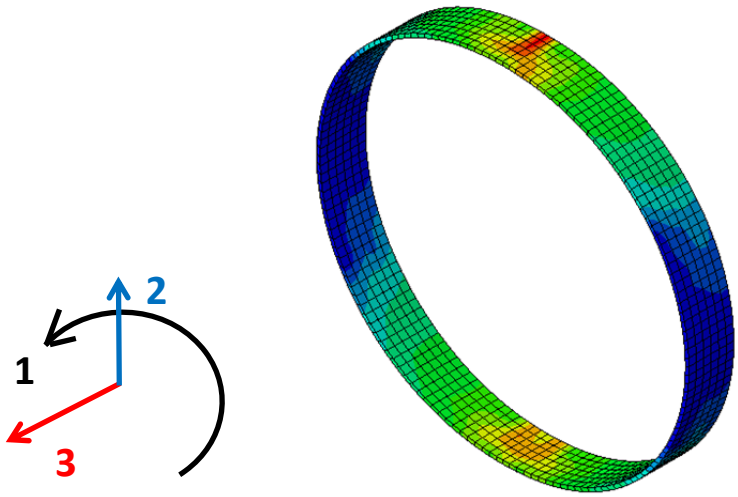

Figure 3.19 Modeled mortar coating

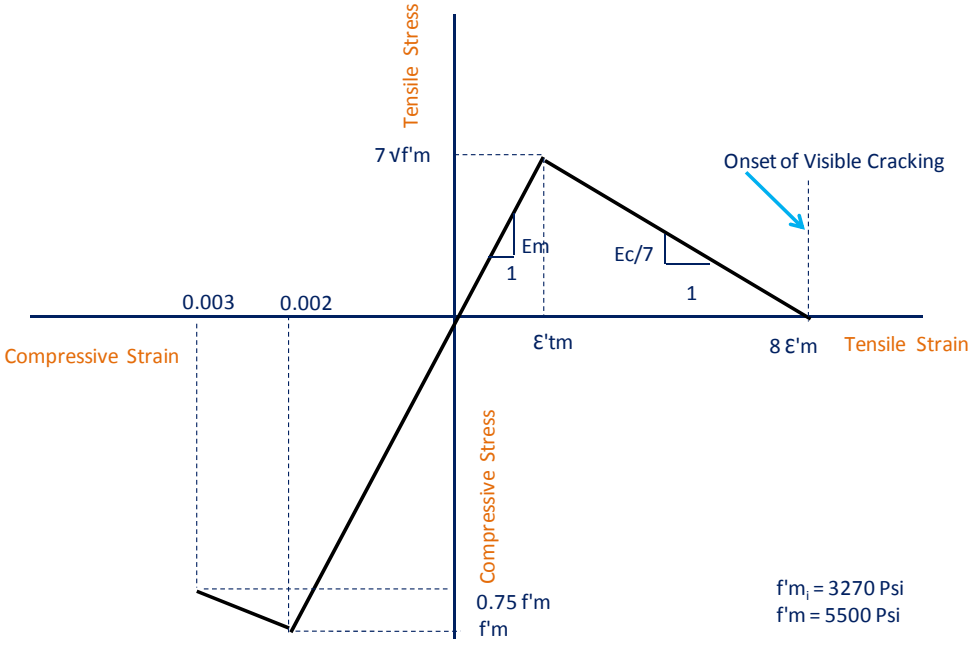

Figure 3.20 Material properties of mortar coating

3.5.2 Contact Modeling

Since PCCP-ECP is a composite with complex stress phenomenon, contacts between the components are crucial factor in governing the PCCP-ECP behavior. Therefore, contacts between each component are carefully modeled, which are subdivided as follows.

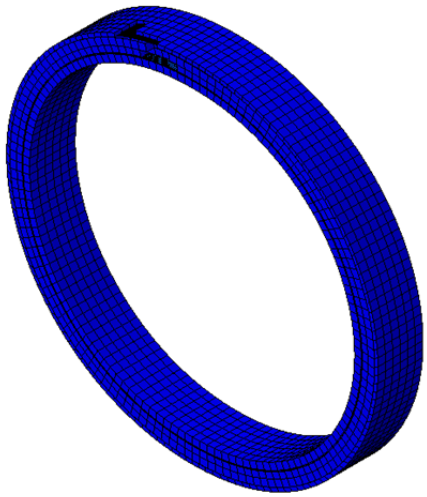

Figure 3.21 PCCP-ECP model

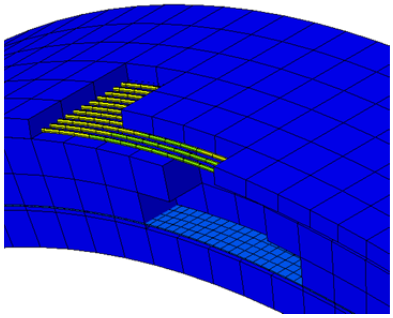

Figure 3.22 Contact between PCCP-ECP components

3.5.2.1 Concrete core and steel cylinder

The concrete core is modeled as host material, and the steel cylinder is modeled as embedded material. The steel cylinder is restrained from any displacement and rotation relative to concrete core in all directions, which are shown in figures 3.21 and 3.22. This simulates the bond between concrete core and steel cylinder.

3.5.2.2 Concrete core and pre-stressing wire

The contact between concrete core and prestressing wire is defined as hard in normal direction and frictionless in tangential direction, which is shown in Figure 3.21. The cross-sectional area of prestressing wire is very small, and when it is wrapped on concrete core, only a thin line of wire comes in contact with concrete core. Since the contact area is negligible, it is reasonable to consider frictionless contact in tangential direction. Also, prestressing wire is wrapped on concrete core only after concrete hardens and reaches minimum required strength. Therefore, it is acceptable to consider as hard in normal direction.

3.5.2.3 Concrete core and mortar coating

The contact between concrete core and mortar coating is considered as hard in normal direction and friction is considered in tangential direction. When the mortar coating is applied on the top of concrete core after prestressing, the bond between two layers ties each other. However, the spacing between prestressing wires, called pitch, is small enough to reduce the contact area between concrete core and mortar coating. This causes the delamination of mortar coating from concrete core during severe external load; for example, three-edge bearing test. High coefficient of friction in tangential direction between concrete core and mortar coating allows separation after cracking of mortar coating. Therefore, it is reasonable to consider hard contact in normal direction and high friction in tangential direction between these layers.

3.5.2.4 Prestressing wire and mortar coating

The prestressing wire is considered as embedded in mortar coating. When mortar coating is applied on the top of prestressed concrete core, the mortar coating is in not in hardened state. When it hardens, prestressing wire is embedded in mortar coating. This simulation allows considering the interaction between relaxation of wire and shrinkage and creep of mortar coating.

3.5.3 Step Modeling

The simulation of manufacturing of PCCP-ECP can be mainly subdivided into four steps: casting of concrete core with embedded cylinder; wrapping of prestressing wire;

equilibrium; and final stage. All the PCCP components, material properties and contact properties are created before modeling the manufacturing steps.

3.5.3.1 Concrete core with embedded cylinder

This is the first step of PCCP-ECP modeling. At this stage, concrete core is assumed to reach minimum required strength. The steel cylinder is embedded into concrete core with considering appropriate contact between these layers as explained above. Since prestress is not applied at this stage, no any kind of prestress loss is considered. Also, mortar coating is deactivated in this step.

3.5.3.2 Wrapping of prestressing wire

At this stage, initial stress is assigned to prestressing wire, which is equal to gross wrapping stress during prestressing. The wire is considered as stretched and wrapped on the concrete core, but it is not clamped to the concrete core. The appropriate contact between concrete core and prestressing wire is assigned as explained above.

3.5.3.3 Equilibrium stage

At this stage, prestressing wire is clamped to the concrete core. Consequently, prestress force is transferred to mortar coating and, the elastic shortening of prestressing wire and concrete core diameter are started. This step continues until the equilibrium between concrete core and prestressing wire reaches. This stage also simulates the effect of compression on steel cylinder.

3.5.3.4 Final stage

At this stage, mortar coating is activated with appropriate contact behavior as explained above. Also, negative temperature is applied to concrete to simulate prestress loss due to shrinkage and creep, and time dependent property is defined to simulate relaxation. The appropriate contact behavior as explained above is assigned to it. This stage simulates the interaction between all components of PCCP-ECP.

3.5.4 Prestress loss Modeling

The main prestress losses in PCCP-ECP are elastic shortening, shrinkage, creep, and relaxation. The shrinkage strain, creep coefficient, and relaxation factor are calculated using equations recommended by AWWA C304 standard, which are given in Appendix A.

3.5.4.1 Elastic shortening

When pipe is wrapped with prestressing wire, it is subjected to radial compressive force. Consequently, pipe diameter reduces, and it causes the reduction in stretched length of the prestressing wire. As a result, stress in prestressing wire decreases, which is termed as prestress loss due to elastic shortening. Although this loss can be calculated by static equations, three dimensional finite element model gives more accurate result since the wire is helical. In addition, it considers the interaction between concrete core and prestressing wire in both tangential and normal directions. Therefore, this loss has been incorporated within the model.

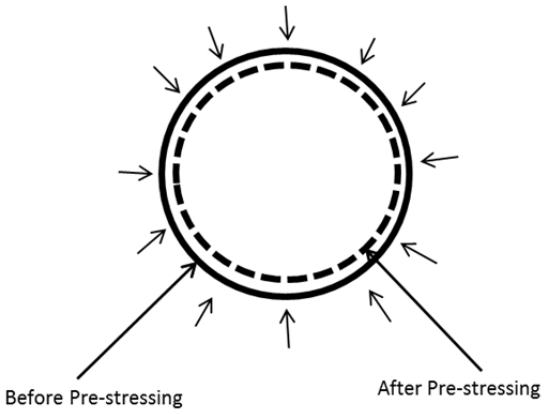

Figure 3.23 Reduction in diameter of pipe due to elastic shortening

3.5.4.2 Shrinkage and creep modeling

Shrinkage is reduction in volume of concrete due to hardening. Similarly, creep is reduction in volume of concrete due to sustain loading in compression. The sustain loading in compression in PCCP-ECP is prestressing force. Therefore, both shrinkage and creep cause reduction in volume of concrete. The loss due to shrinkage and creep are calculated by

following equations given in Appendix A. Negative temperature is applied to concrete to simulate shrinkage and creep loss.

3.5.4.3 Relaxation modeling

Relaxation is caused due to loss in stress of prestressing wire at constant length and temperature. This loss in stress causes increase in pipe diameter, which reduces the compression in core, and is termed as prestress loss due to relaxation. The effect of relaxation is simulated by defining the time dependent properties of prestressing wire, which is given in Appendix A.

3.5.5 Three-Edge Bearing Modeling

The PCCP-ECP model is loaded as in three-edge bearing test. The lower and upper bearings are modeled as rigid body so that no deformation within bearing takes place. The PCCP-ECP model is loaded with constant rate of vertical displacement. The PCCP-ECP is loaded through its top bearing, and simulated test is performed approximately to four percent of vertical deflection. The simulated test is displacement controlled test, which means displacement is applied to the top bearing to generate load on the pipe, which is shown in Figure 3.24.

Figure 3.24 Three-edge bearing model

The load versus percentage vertical deflection is plotted from the data obtained from finite element model test, which is shown in Figure 3.25.

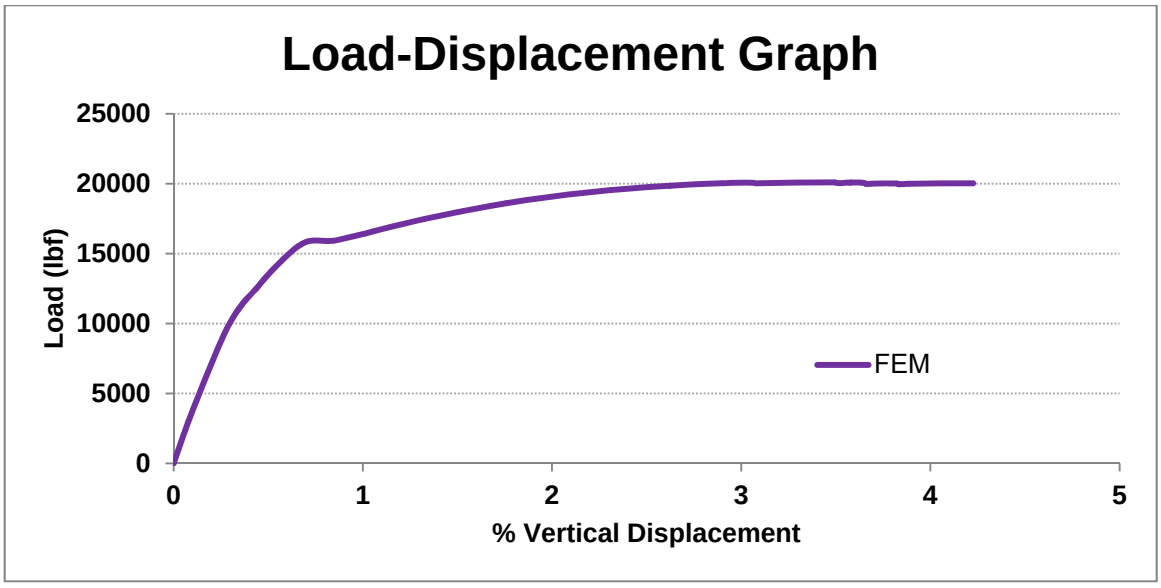

Figure 3.25 Load-displacement graph obtained from finite element modeling

CHAPTER-4

RESULTS AND CONCLUSION

4.1 Results

The comparison between results obtained from experiment and finite element modeling is done to validate the model. The experiment is conducted on two PCCP-ECPs as explained in the experiment chapter. In both tests, the length of PCCP-ECPs were 5.5 feet. Since the finite element modeling is conducted on 1 foot PCCP, the experiment results are converted to equivalent of 1 foot PCCP-ECP so that comparison between results obtained from experiment and finite element modeling can be done.

4.1.1Experiment

The vertical load carrying capacity of pipe increases with increase in length of the pipe. The loads obtained from the experiment are converted to load per foot of the pipe by dividing the loads by length of the PCCP-ECP.

4.1.1.1 Load-crack log

The load and corresponding crack widths given in Table 4.1 are for 1 foot length of PCCP-ECP. It can be seen that the first incipient crack occurred at 15.64 kips load at invert. The ninety percent of load that causes 0.001 inch cracking without internal pressure is 14.07 kips for the tested PCCP-ECP.

Table 4.1 Load and corresponding crack widths for 1 foot length of PCCP

Load (kips)	**Observed**
3.64	No Cracks
5.45	No Cracks
7.27	No Cracks
9.09	No Cracks; vertical deflection suddenly increased
10.91	No Cracks
12.73	No Cracks
13.64	No Cracks
14.00	No Cracks
14.55	No Cracks
15.64	First crack at invert; 0.001 inch
16.36	Another 0.001 inch crack near invert
16.36	0.001 inch crack at crown
17.27	0.01 inch crack at invert
17.64	separation of mortar coating from concrete core started
18.18	0.016 inch crack at crown
18.18	0.02 inch crack at invert
18.18	hair line crack at spring line
20.00	0.06 inch crack at crown
20.00	0.05 inch crack at invert
20.00	0.016 inch crack at spring line

4.1.1.2 Load-displacement graph

The load-displacement graphs of one foot PCCP-ECP obtained from experiment 1 and experiment 2 are given in Figure 4.1 and Figure 4.2 respectively. It can be seen that both experiment results are showing similar nature of curve. The rate of increase of load with respect to displacement is very high up to around 0.5% vertical displacement. Also, there is almost no change in load after 3% vertical displacement.

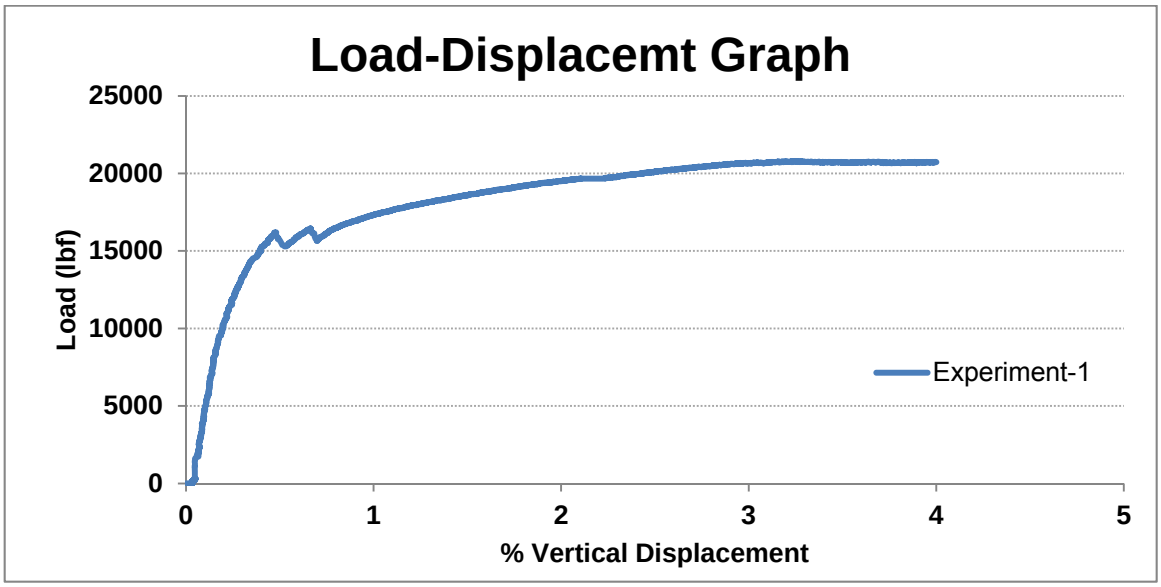

Figure 4.1 Load-displacement graph from Experiment 1

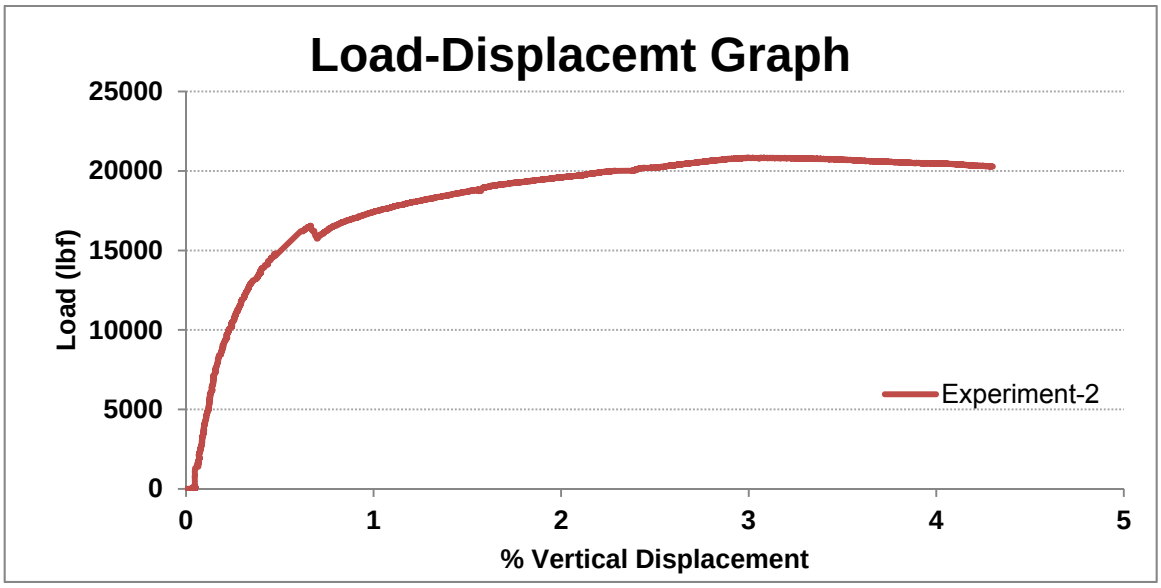

Figure 4.2 Load-displacement graph from Experiment 2

4.1.2 Finite Element Model

4.1.2.1 Load-displacement graph

The load-displacement graph obtained from finite element modeling is given below in Figure 4.3. It can be seen that the rate of increase of load with respect to displacement is very high up to around 0.5% vertical displacement. Also, there is almost no change in load after 3% vertical displacement.

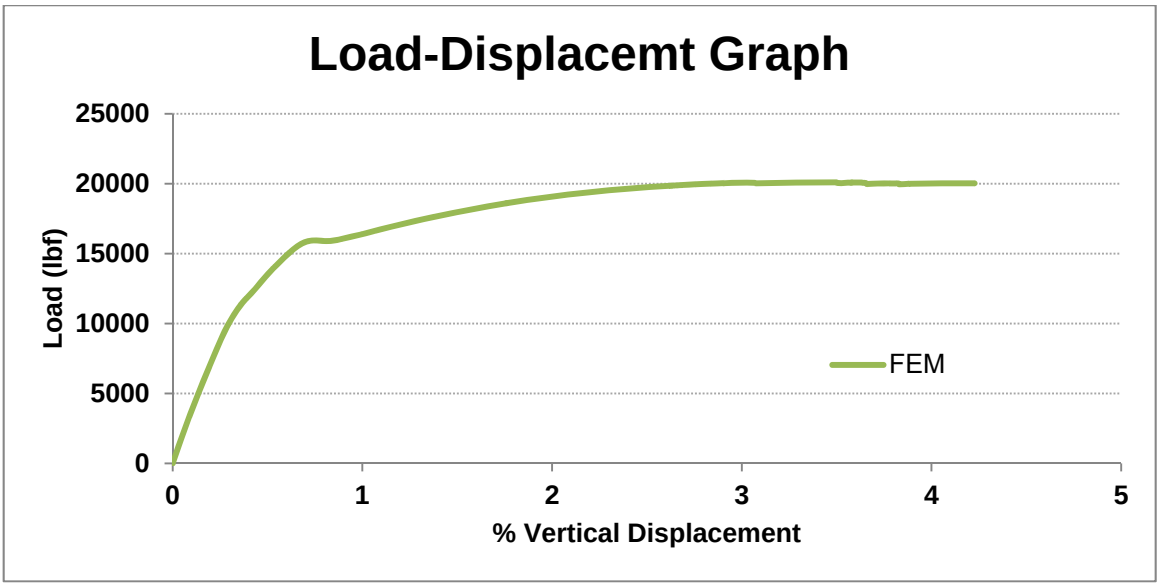

Figure 4.3 Load-displacement graph from FEM

4.2 Discussion

4.2.1 Comparison of load-displacement

The comparison of load-displacement graph obtained from Experiment 1, Experiment 2, and FEM is shown in the Figure 4.4. It can be seen that both experiments results are overlapping, which indicates that the experiments were carefully conducted. Also, the result obtained from FEM is closely following the experiment results. This validates the accuracy of finite element modeling of PCCP-ECP.

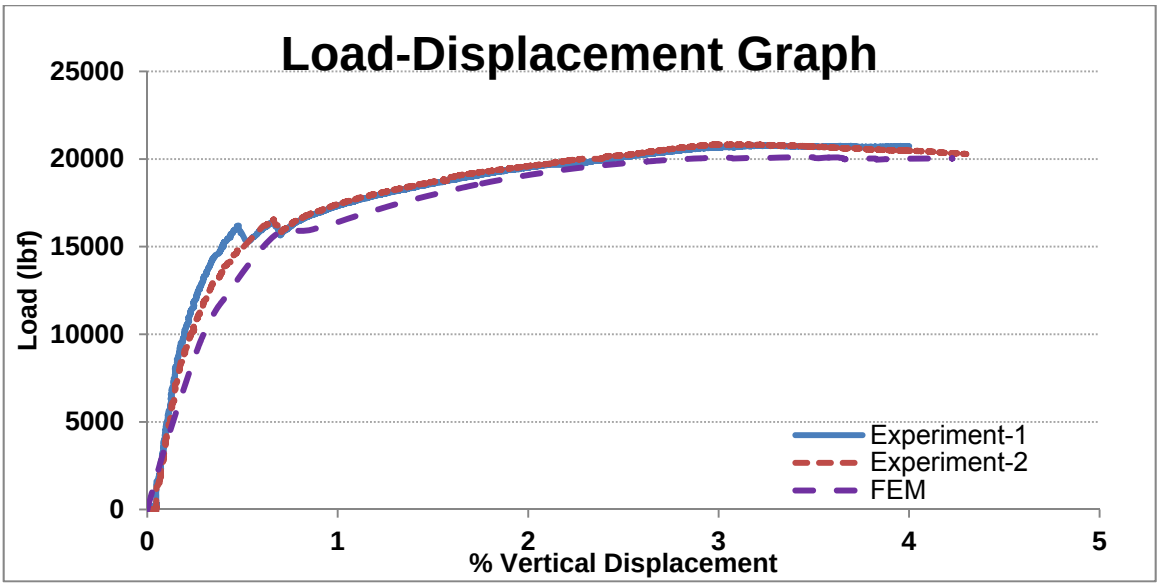

Figure 4.4 Comparison of Load-displacement graph from Experiments and FEM

4.2.2 Comparison of stress

The stress in concrete core, steel cylinder, prestressing wire, and mortar coating obtained from finite element modeling at initial and final prestress are compared with the stress obtained from equations in AWWA C034 standard. The stresses are plotted at 45 degree angle locations, which are main points of interest. The detail calculation of stress obtained from AWWA C304 equations can be seen in the Appendix A.

4.2.2.1 stress in concrete core

The stresses in concrete core at initial and final prestress are shown in figure 4.5. The stress obtained are slightly less than that from AWWA C304 equations. The reason for this is AWWA C304 uses wrapping stress to calculate the initial stress; however, it is less in reality due to elastic shortening of pipe.

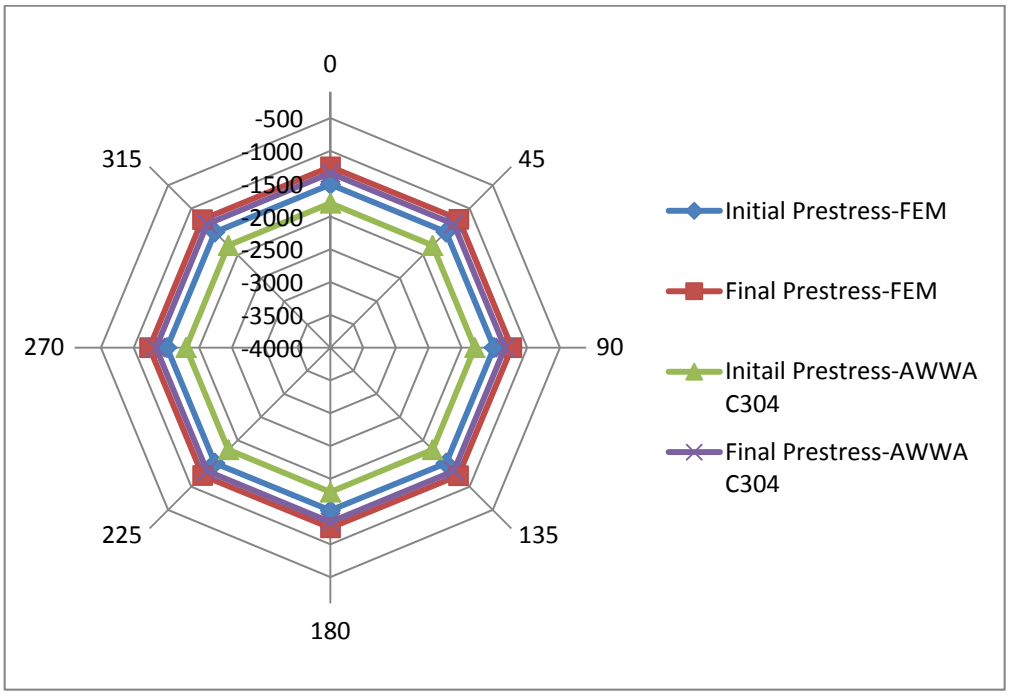

Figure 4.5 Comparison of stress in core

4.2.2.2 stress in steel cylinder

The stresses in steel cylinder at initial and final prestress are shown in figure 4.6. The stress obtained are slightly less than that from AWWA C304 equations.

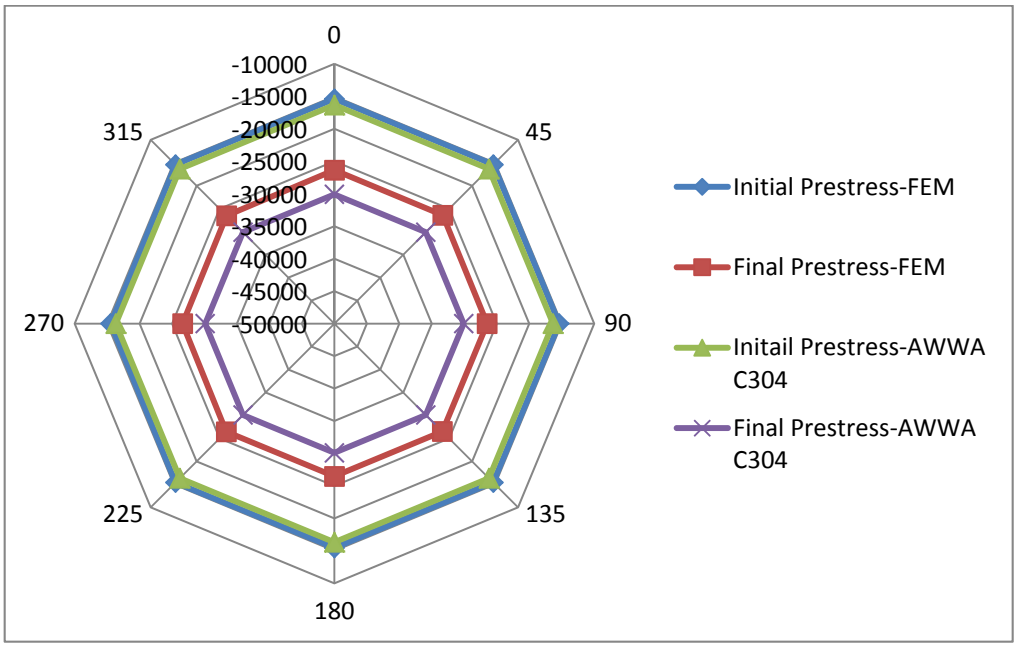

Figure 4.6 Comparison of stress in steel cylinder

4.2.2.3 Stress in prestressing wire

The stresses in prestressing wire at initial and final prestress are shown in figure 4.7. The stress obtained are slightly more than that from AWWA C304 equations.

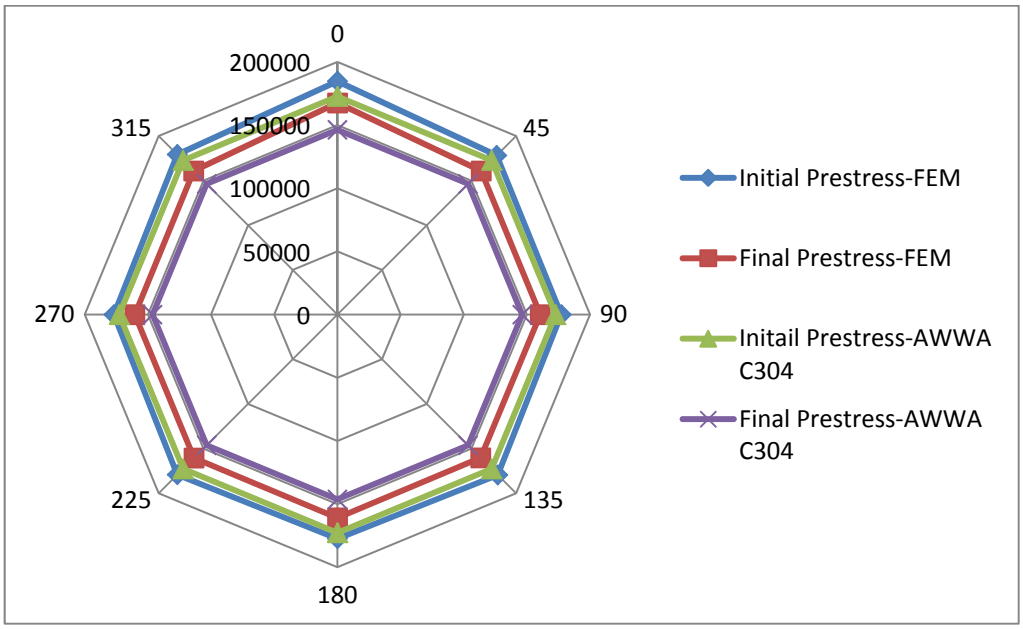

Figure 4.7 Comparison of stress in prestressing wire

4.2.2.4 stress in mortar coating

The stress in mortar coating at final prestress is shown in figure 4.8.

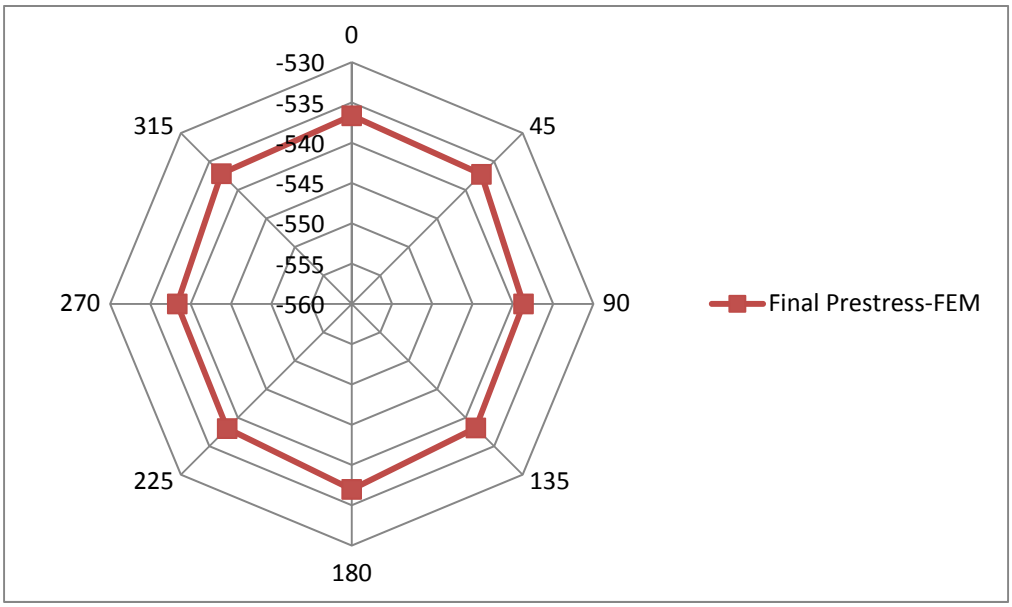

Figure 4.8 Stress in mortar coating

4.2.3 Stress at different stage during three-edge bearing

The stress in concrete core, steel cylinder, prestressing wire, and mortar coating at different stage during three edge bearing test of model are shown. The load-displacement graph is also plotted with stress so that behavior of pipe can be better analyzed. The stress are plotted for the points on the circumference at 45 degree interval. The points include invert, crown, springline at 45 degree or 3 o' clock position, and springline at 270 degree or 9 o' clock position, which are crucial points. The value in the left axis is load during three-edge bearing, and value in the right axis is stress in the PCCP-ECP elements at different locations.

4.2.3.1 stress in concrete core

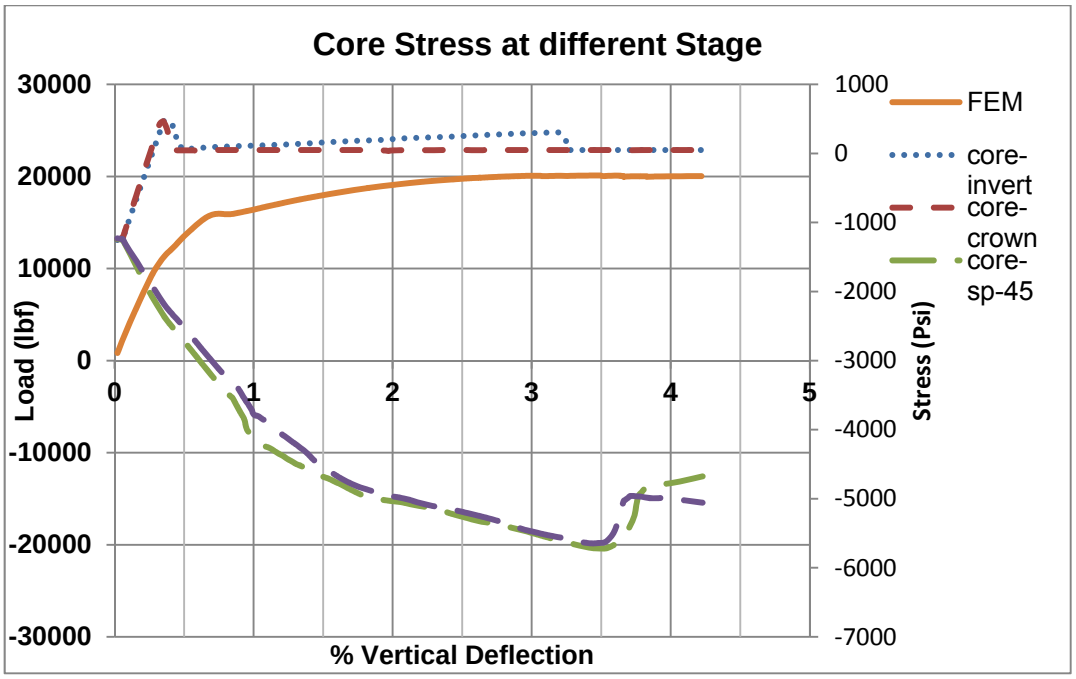

Figure 4.9 Stress in core at different loading stages

4.2.3.2 stress in steel cylinder

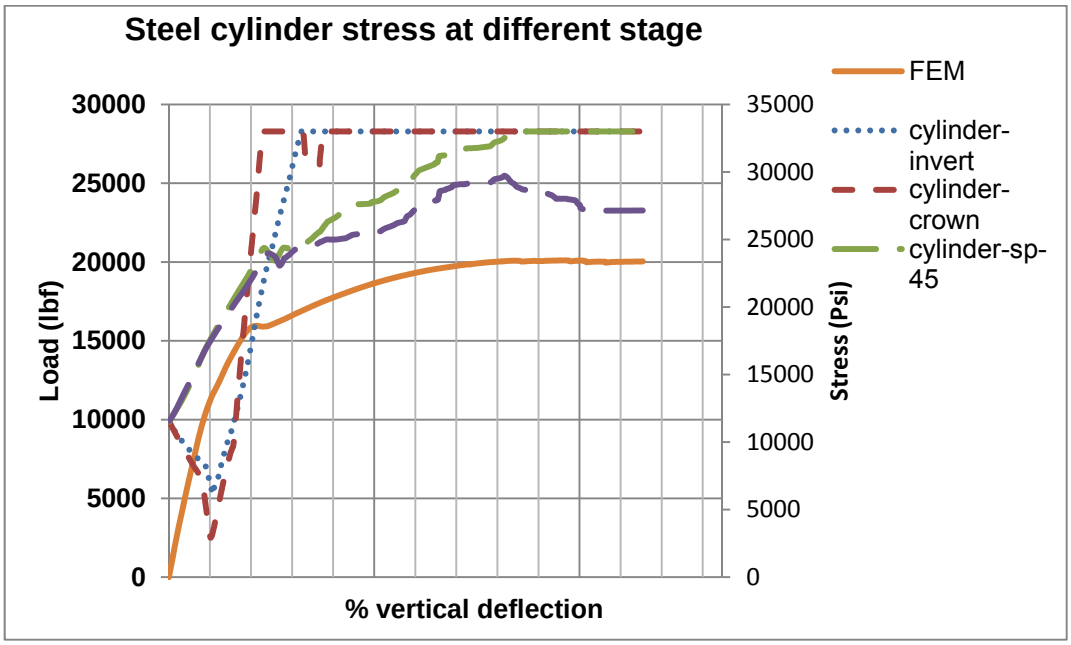

Figure 4.10 Stress in steel cylinder at different loading stages

4.2.3.3 stress in prestressing wire

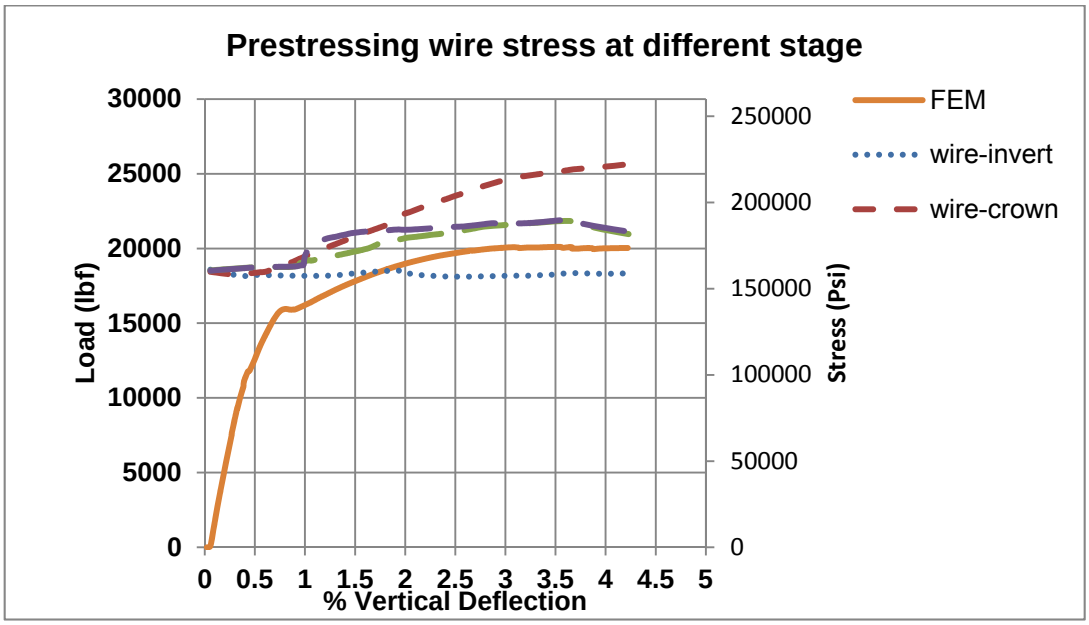

Figure 4.11 Stress in prestressing wire at different loading stages

4.2.3.4 stress in mortar coating

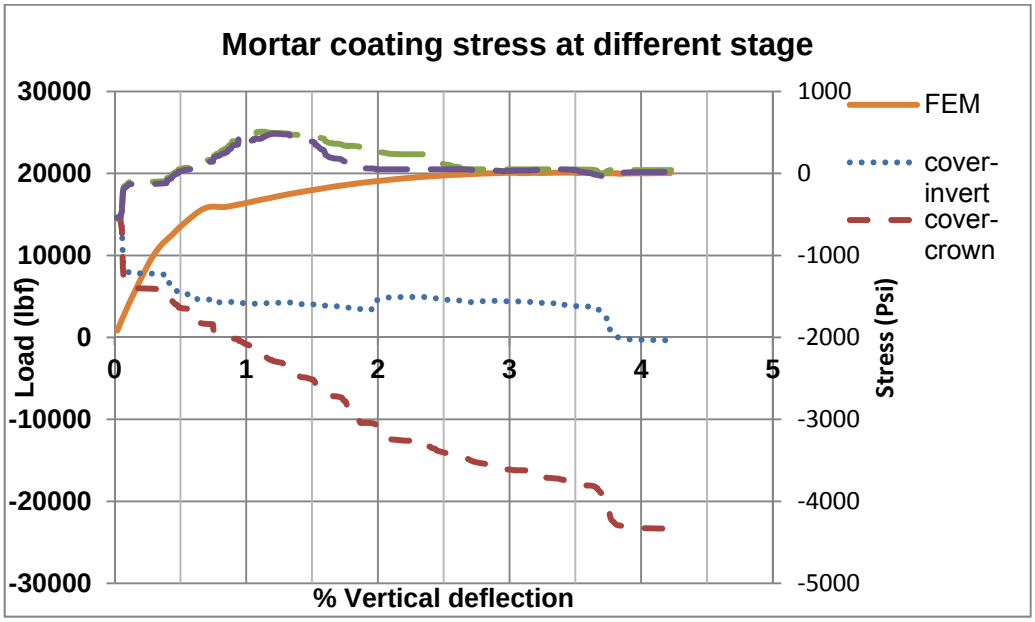

Figure 4.12 stress in mortar coating at different loading stage

4.3 Summary

PCCP-ECP is a composite pipe consisting of concrete core, steel cylinder, prestressing wire, and mortar coating. Concrete undergoes shrinkage and creep, and its strength is a function of time. In addition, prestressing force and relaxation of prestressing wire causes the interaction between components more complicated. However, analysis of PCCP-ECP is important to understand the PCCP-ECP behavior.

PCCP-ECP is pressure pipe, and failure of PCCP-ECP is of disastrous nature. In addition, maintenance and replacement of PCCP-ECP is very costly. The current design procedure of PCCP-ECP in pipe industry is done by following AWWA C304 standard. The design procedure in AWWA C304 is based on limit state method. The equations used for calculating initial and final prestress are based on step by step integration method. Moreover,

the design procedure in AWWA C304 considers the Olander coefficients to calculate the shear and moment, which are based on elastic analysis. However, PCCP-ECP consists of different components and interaction between components is crucial to analyze the simultaneous effect of prestress loss and stress in each components.

A three dimensional model of PCCP-ECP is created by considering non-linearities due to geometry, material properties, large deformation, and interaction between each components. Two full scale three edge bearing test were conducted in real PCCP-ECP to observe the real PCCP-ECP behavior. The model is used to analyze the stress and role of each components in PCCP-ECP. The model can be used to analyze the PCCP-ECP in different scenario.

4.4 Conclusion

A three dimensional model of PCCP-ECP is created to simulate the real pipe behavior by considering the contribution of all components of PCCP-ECP. Two full scale three-edge bearing tests were conducted to understand the real PCCP-ECP behavior. The three-edge bearing test was also done on the modeled PCCP-ECP to validate the modeled PCCP-ECP. The load-displacement graph obtained from experiment and finite element model shows good agreement between results. The modeled PCCP-ECP can be used for analysis for any loading case.

The analysis of modeled PCCP-ECP concludes that stress in prestressing wire varies due to external loads. It also concludes that although the steel cylinder is assumed as non-structural element in PCCP-ECP, it plays role in load bearing behavior of PCCP-ECP. Also, the stiffness of PCCP-ECP suddenly decreases after cracking of core.

The modeled PCCP-ECP gives very accurate stress in each component. The modeled PCCP-ECP can be used to simulate pipe behavior at stage construction during installation of pipe. This would help to save cost of real pipe test. Any potential failure of PCCP-ECP due to any reason can be analyzed before it happens in reality. This model could be very good tool to perform case study of PCCP-ECP failures.

4.5 Recommendation

This paper limits the analysis of PCCP- ECP for single layer of prestressing wire, which is more common in practice. However, when the prestressing force required is high and pitch of prestressing wire exceeds the minimum spacing requirement, multiple layers of prestressing wire is required. Therefore, further research is recommended to analyze the PCCP-ECP behavior for multiple layer of prestressing wire case.

APPENDIX A

CALCULATION OF STRESS AND PRESTRESS LOSS

A.1: Calculation

A.1.1: Properties

Unit weight of concrete,

$$\gamma_c = 145\ lb/ft^3$$

Compressive strength of concrete at maturity,

$$f_c = 5000\ psi$$

Compressive strength of concrete at wrapping,

$$f_{ci} = 3270\ psi$$

Area of prestressing wire per foot of pipe,

$$A_s = \frac{\pi}{4} \times d_s^2 = 0.172\ in^2$$

Gross wrapping stress of prestressing wire,

$$f_{sg} = 189000\ psi$$

Area of concrete core per foot excluding steel cylinder,

$$A_c = (h_c - t_s) \times 12\ in^2$$

Area of steel cylinder per foot of the pipe,

$$A_y = t_s \times 12 = 0.0598 \times 12\ in^2$$

Modulus of elasticity of Prestressing wire,

$$E_s = 28 \times 10^6\ psi$$

Modulus of elasticity of steel cylinder

$$E_y = 30 \times 10^6\ psi$$

Inner core thickness

$$h_{ci} = 1.9402\ in.$$

Outer core thickness,

$$h_{co} = 3.25\ \ in.$$

Mortar coating thickness,

$$h_m = 0.942\ \ in.$$

Outside diameter of steel cylinder,

$$D_y = 88\ \ in.$$

Relative humidity,

$$RH = 70\%$$

Duration of pipe exposed to an outdoor environment with humidity RH,

$$t_1 = 90\ days$$

Duration of pipe exposed to a burial environment with 92.5 %humidity,

$$t_2 = 0\ days$$

A.1.2: Creep factor

$$\rho = 0.8$$

$$\emptyset_1 = 2.35\left[\frac{\rho - 0.65}{1 + 10/t_1^{0.6}} + \frac{0.05}{1 + 10/(t_1 + t_2)^{0.6}} + 0.6\right] = 1.691$$

$$\emptyset_2 = 2.35\left[\frac{\rho - 0.65}{1 + 10/t_1^{0.6}} + 0.6\right] = 1.621$$

$$\gamma(h) = \frac{2}{3}(1 + 1.13 \times e^{-0.54h})$$

$$\emptyset_{ci} = \emptyset_1 \times \gamma(h_{ci})$$

$$\emptyset_{com} = \emptyset_2 \times \gamma(h_{co} + h_m)$$

$$\emptyset_m = \emptyset_2 \times \gamma(h_m)$$

$$\emptyset = \frac{(h_{co} + h_m)\emptyset_{com} - h_m\emptyset_m + h_{ci}\emptyset_{ci}}{h_{ci} + h_{co}}$$

$$\emptyset = 1.234$$

A.1. 3: Shrinkage strain

$$\rho' = 0.7$$

$$S_1 = 312 \times 10^{-6}\left[\frac{(\rho' - 0.225)t_1}{t_1 + 55} + \frac{0.225(t_1 + t_2)}{t_1 + t_2 + 55}\right] = 1.356 \times 10^{-4}$$

$$S_2 = 780 \times 10^{-6}\left[\frac{(0.4\rho' - 0.09)t_1}{t_1 + 55} + 0.225\right] = 2.675 \times 10^{-4}$$

$$\gamma'(h) = 1.2\, e^{-0.12h}$$

$$S_{ci} = S_1 \times \gamma'(h_{ci})$$

$$S_{com} = S_2 \times \gamma'(h_{co} + h_m)$$

$$S_m = S_2 \times \gamma'(h_m)$$

$$S_{com} - S_m = -1.035 \times 10^{-4}$$

$$S = \frac{(h_{co} + h_m)S_{com} - h_m S_m + h_{ci} S_{ci}}{h_{ci} + h_{co}}$$

$$S = 1.529 \times 10^{-4}$$

A.1. 4: Wire-Relaxation factor

$$R = \left(\frac{\log(24 \times t_p + 1)}{12}\right) \times \left(\frac{f_{sg}}{0.85 f_{su}} - 0.55\right) = 0.076$$

A.1. 5: Concrete strength

$$E_c = 158\gamma_c^{1.51} f_c^{0.3} = 3.733 \times 10^6$$

$$E_{ci} = 158\gamma_c^{1.51} f_{ci}^{0.3} = 3.286 \times 10^6$$

A.1. 6: Ratio of modulus of wire to concrete

At wrapping

$$\eta_i = 109 f_c^{-0.3} = 8.467$$

At maturity

$$\eta_r = 93 f_c^{-0.3} = 7.224$$

A.1. 7: Ratio of modulus of steel to concrete

At wrapping

$$\eta_i{}' = 117 f_c^{-0.3} = 9.089$$

At maturity

$$\eta_r{}' = 99 f_c^{-0.3} = 7.69$$

A.2: Initial Prestress

A.2.1: Concrete core

$$f_{ic} = \frac{A_s f_{sg}}{A_c + \eta_i A_s + \eta_i{}' A_y} = 1.798 \times 10^3$$

A.2.2: Steel cylinder

$$f_{iy}{}' = \eta_i{}' f_{ic} = 1.634 \times 10^4$$

A.2.3: Prestressing wire

$$f_{is} = -f_{sg} + \eta_i' f_{ic} = -1.727 \times 10^5$$

A.3: Final prestress

A.3.1: Concrete core

$$f_{cr} = \frac{f_{ic}(A_c + \eta_r A_s + \eta_r{}'.A_y) - (A_s E_s + A_y E_y)s - A_s R f_{sg}}{A_c + (\eta_r A_s + \eta_r'.A_y)\,(1+\emptyset)}$$

$$f_{cr} = 1.331 \times 10^3$$

$$\varepsilon_{cr} = \frac{f_{cr}}{E_c} = 3.566 \times 10^{-4}$$

A.3.2: Steel cylinder

$$f_{yr} = f_{iy} + \frac{A_c(f_{ic}\emptyset\,\eta_r' + E_y s) - R\,A_s f_{sg}\eta_r{}'(1+\emptyset)}{A_c + (\eta_r A_s + \eta_r'.A_y)\,(1+\emptyset)}$$

$$f_{yr} = 2.997 \times 10^4$$

A.3.4: Wire

$$f_{sr} = f_{is} + R\,f_{sg} + \frac{A_c(f_{ic}\emptyset\,\eta_r + E_s\,s) - R\,A_s f_{sg}\eta_r(1+\emptyset)}{A_c + (\eta_r A_s + \eta_r'.A_y)\,(1+\emptyset)}$$

$$f_{sr} = -1.455 \times 10^5$$

A.4: Decompression pressure

$$P_o = \frac{f_{cr}(A_c + \eta_r A_s + \eta_r{}' A_y}{6D_y} = 183.878$$

A.5: Temperature calculation

A.5.1: Shrinkage:

$$\Delta fps_{SH} = E_s s = 4.282 \times 10^3$$

$$\alpha = 5 \times 10^{-6}$$

$$\Delta T_{SH} = \frac{s}{\alpha} = 30.583$$

This is the negative temperature to apply to concrete

A.5.2: Creep:

$$\sigma_i = \frac{A_s f_{sg}}{(A_c + \eta_i' A_y)12}$$

$$\varepsilon_{ci} = \frac{\sigma_i}{Ec_i} = 4.96 \times 10^{-5}$$

$$\varepsilon_c = \emptyset \varepsilon_{ci} = 6.122 \times 10^{-5}$$

$$\Delta T_{CR} = \frac{\varepsilon_c}{\alpha} = 12.244$$

This is the negative temperature to apply to concrete

$$\Delta T_{SH} + \Delta T_{CR} = 42.827$$

A.5.3: Relaxation:

$$\Delta P_R = R f_{sg} = 1.43 \times 10^4$$

$$f_{sg} - R f_{sg} = 1.746 \times 10^5$$

APPENDIX B

FEM STRESS AT DIFFERENT STAGES

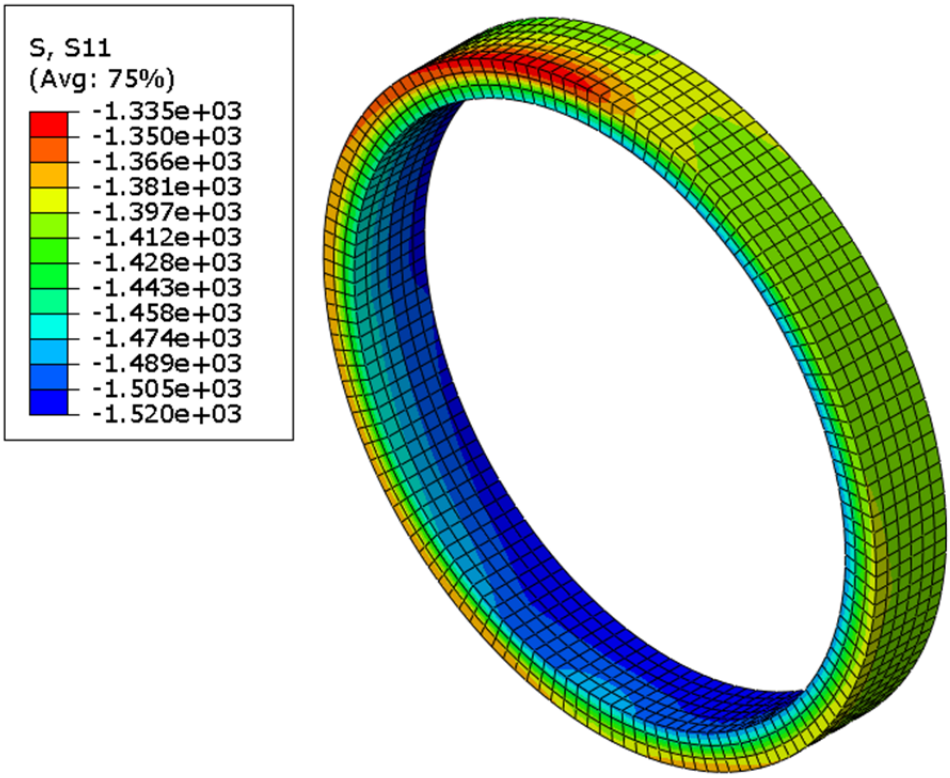

Figure 5.1 Circumferential stress in core at initial prestress

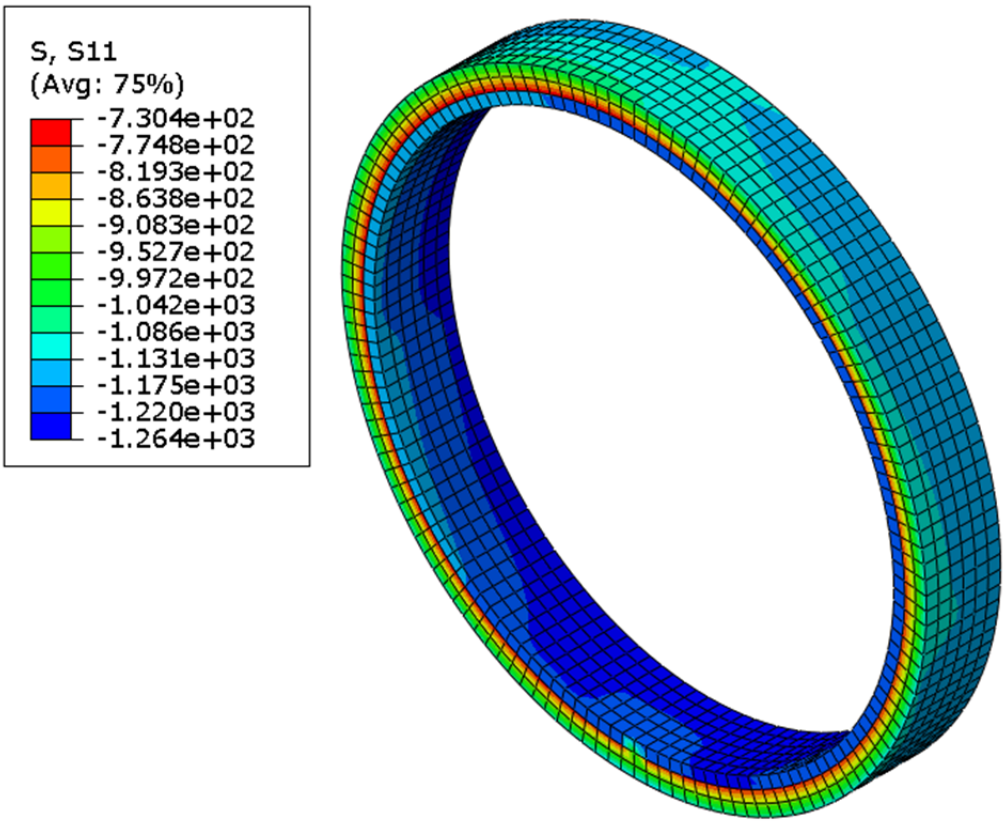

Figure 5.2 Circumferential stress in core at final prestress

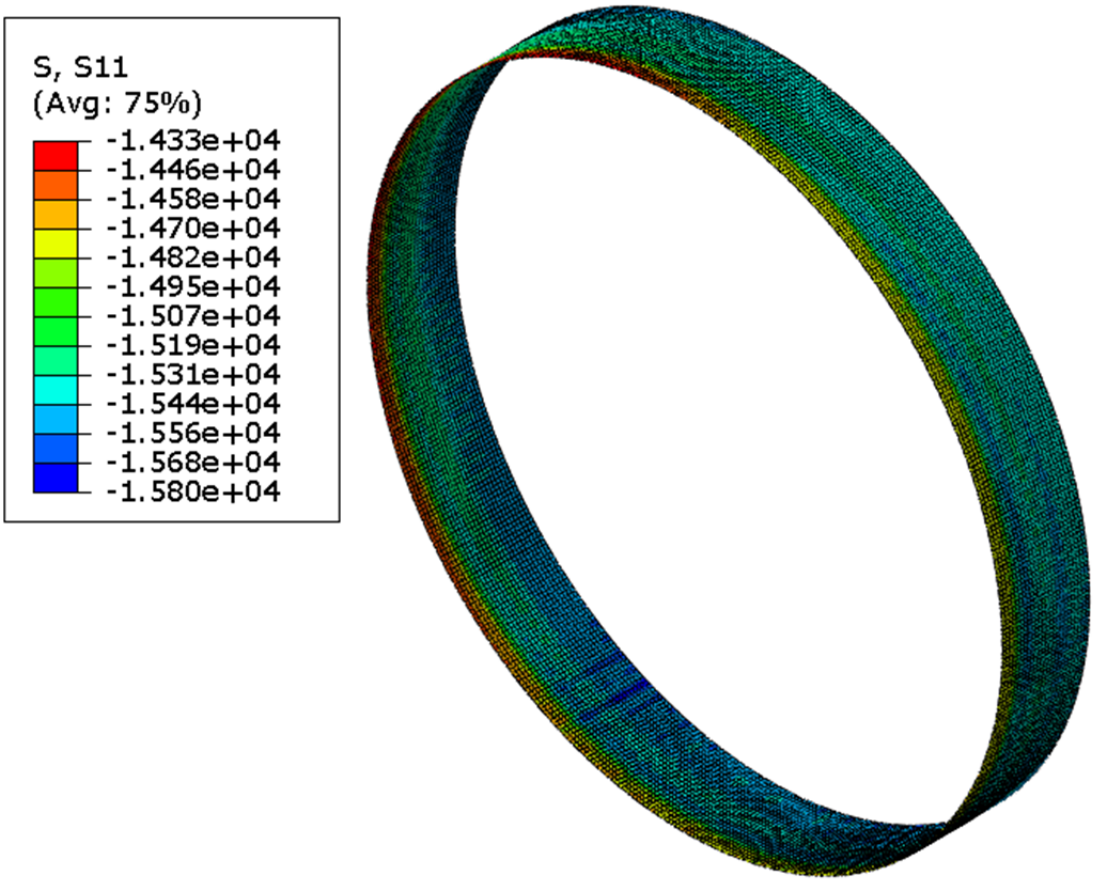

Figure 5.3 Circumferential stress in steel cylinder at initial prestress

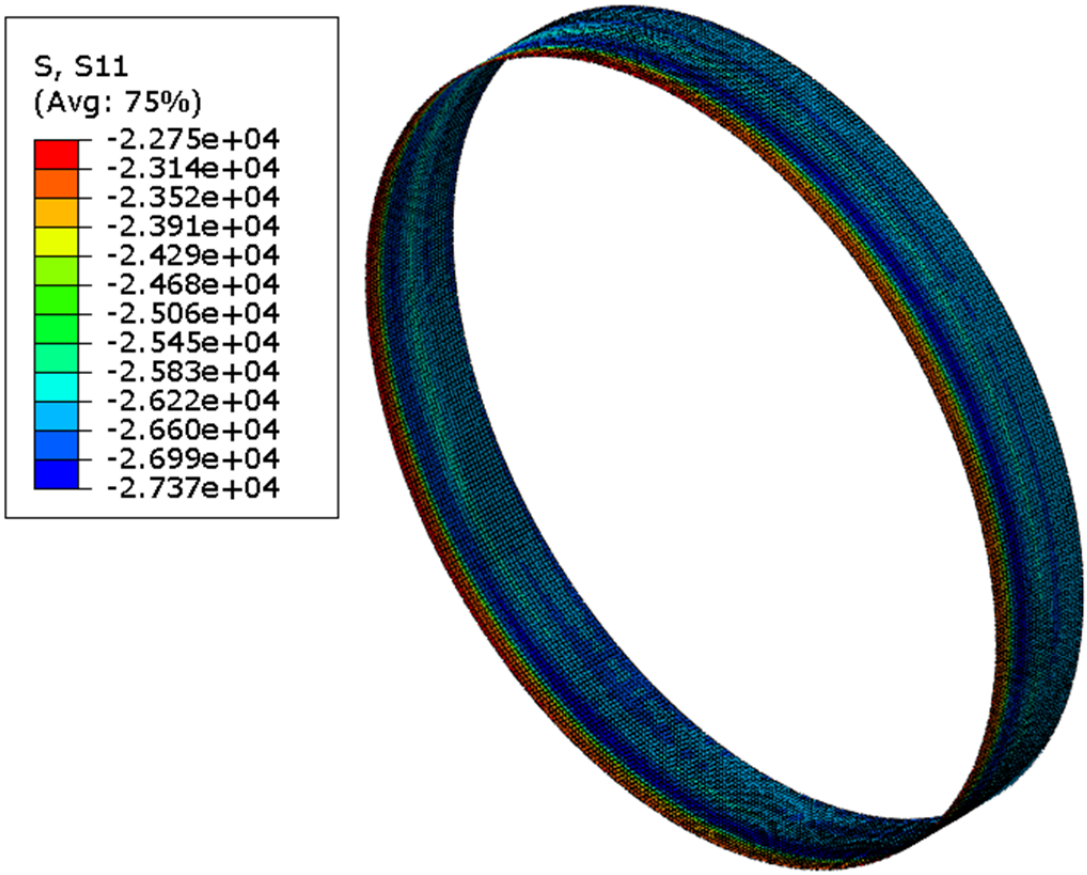

Figure 5.4 Circumferential stress in steel cylinder at final prestress

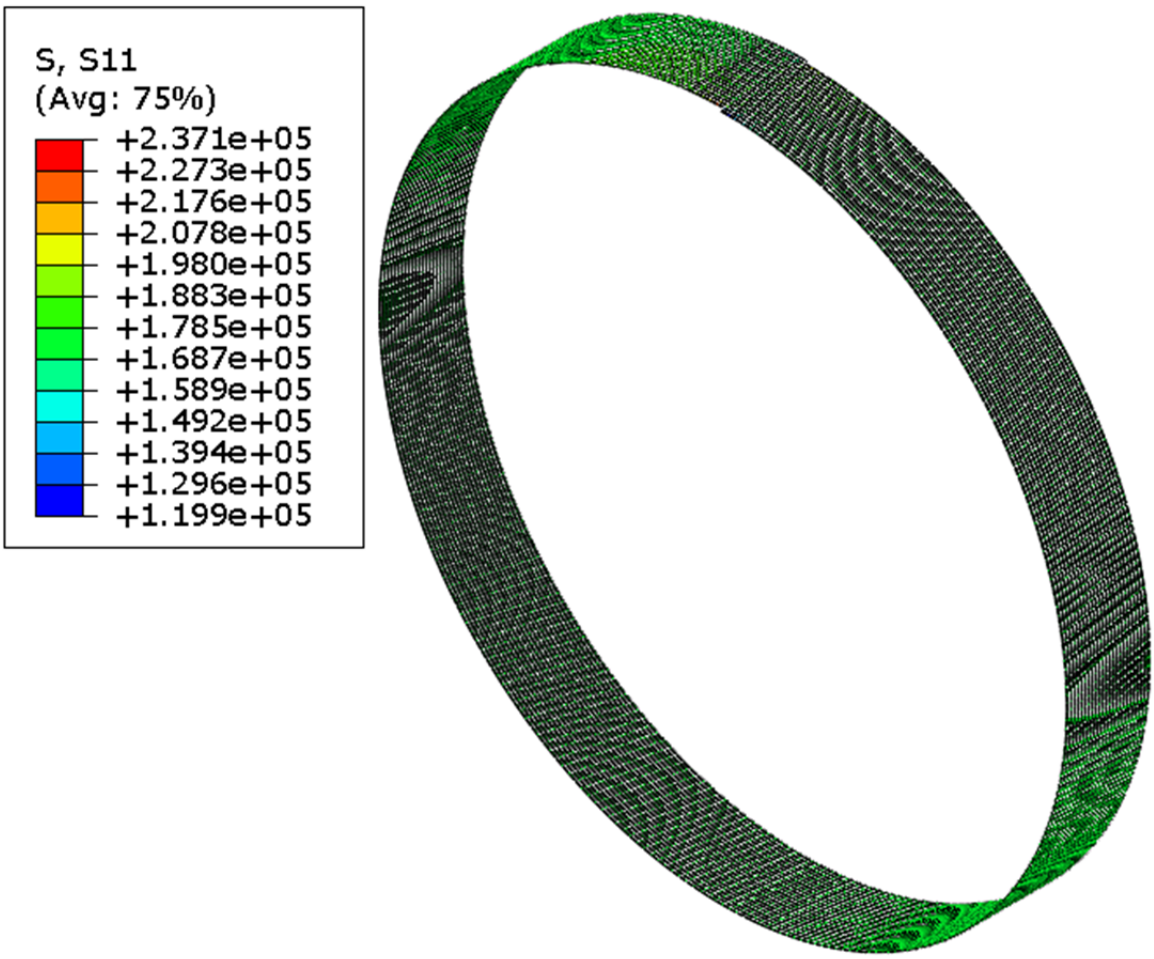

Figure 5.5 Longitudinal stress in prestressing wire at initial prestress

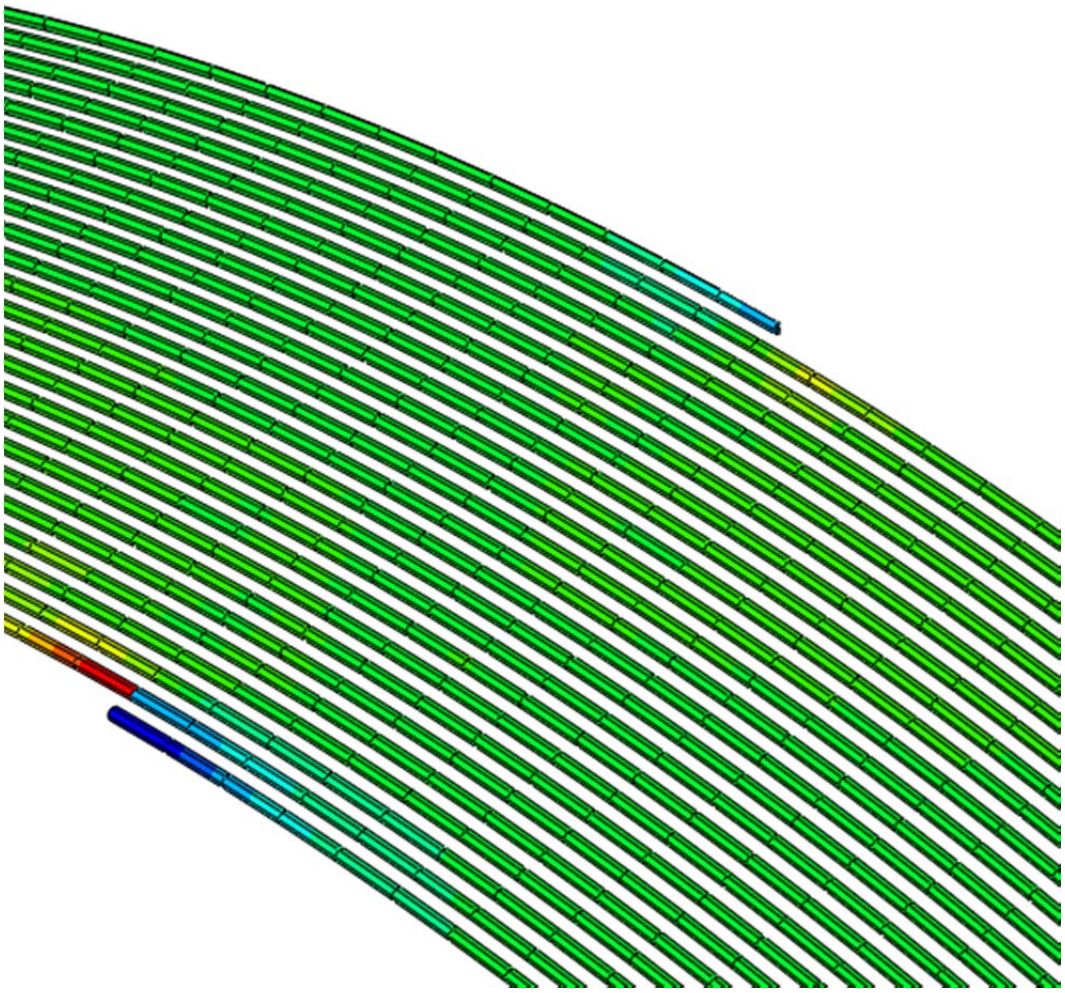

Figure 5.6 Enlarged crown part of figure 5.5

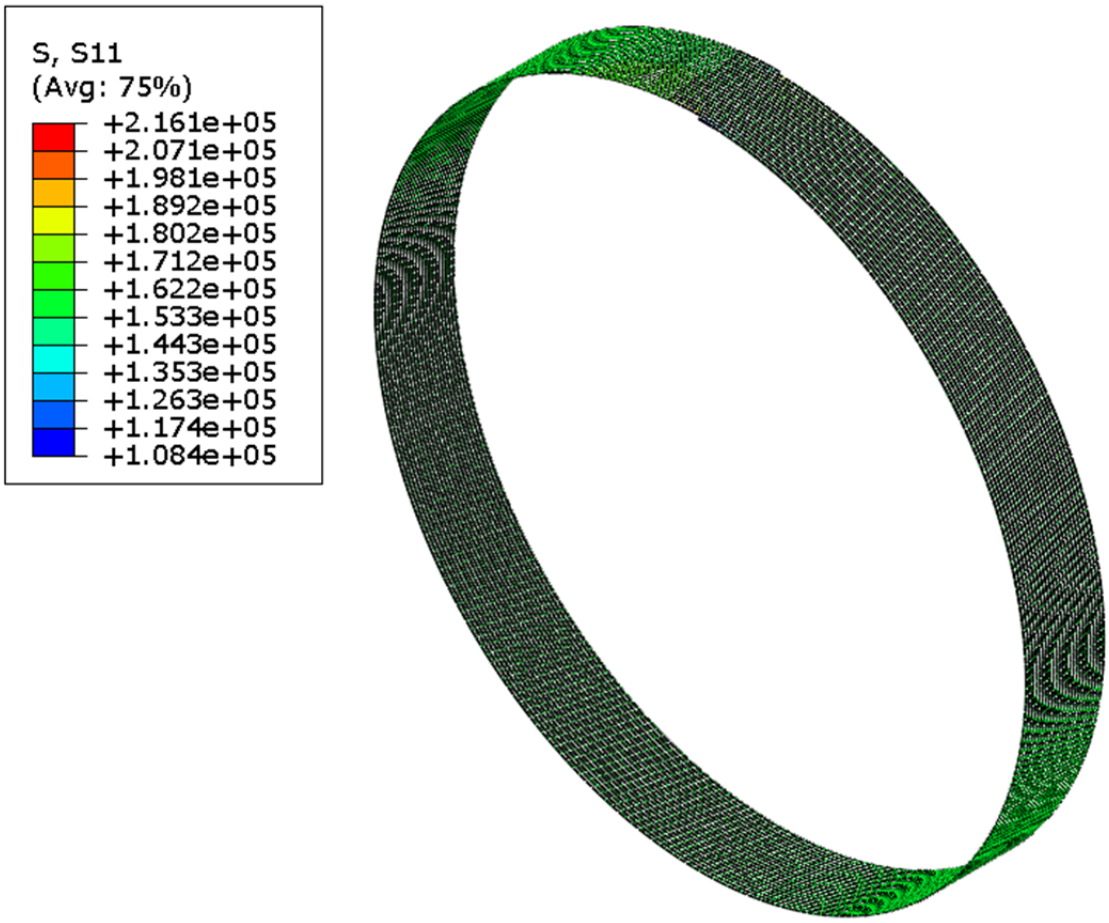

Figure 5.7 Longitudinal stress in prestressing wire at final prestress

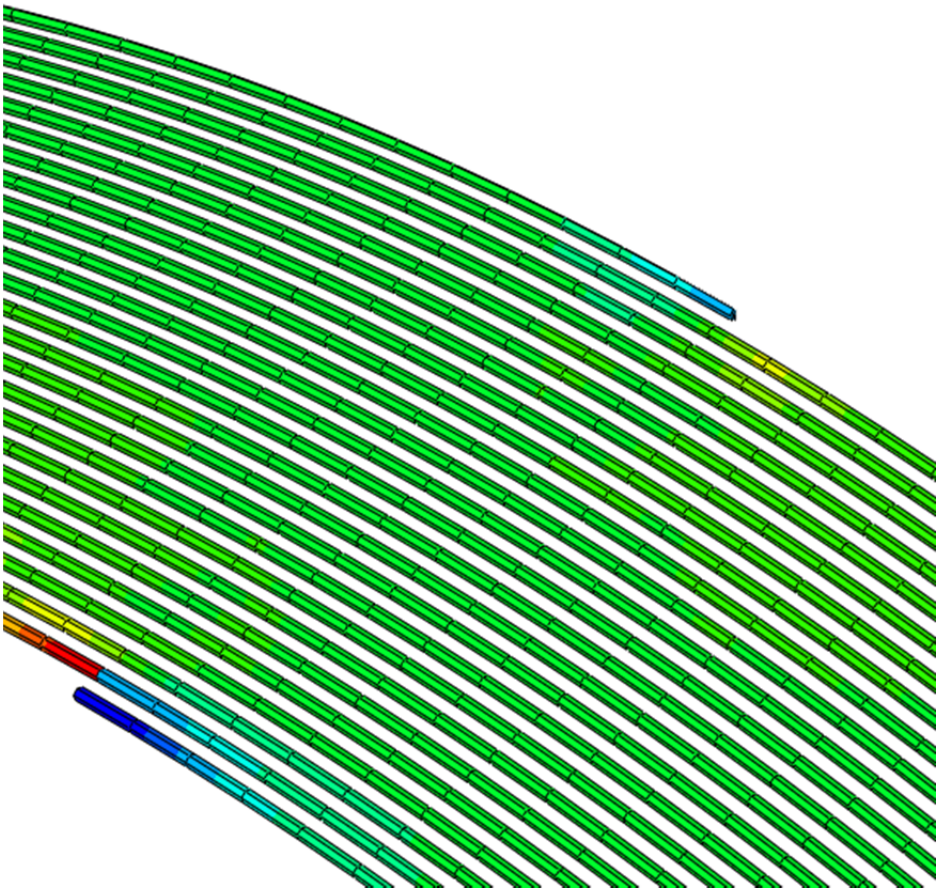

Figure 5.8 Enlarged crown part of figure 5.6

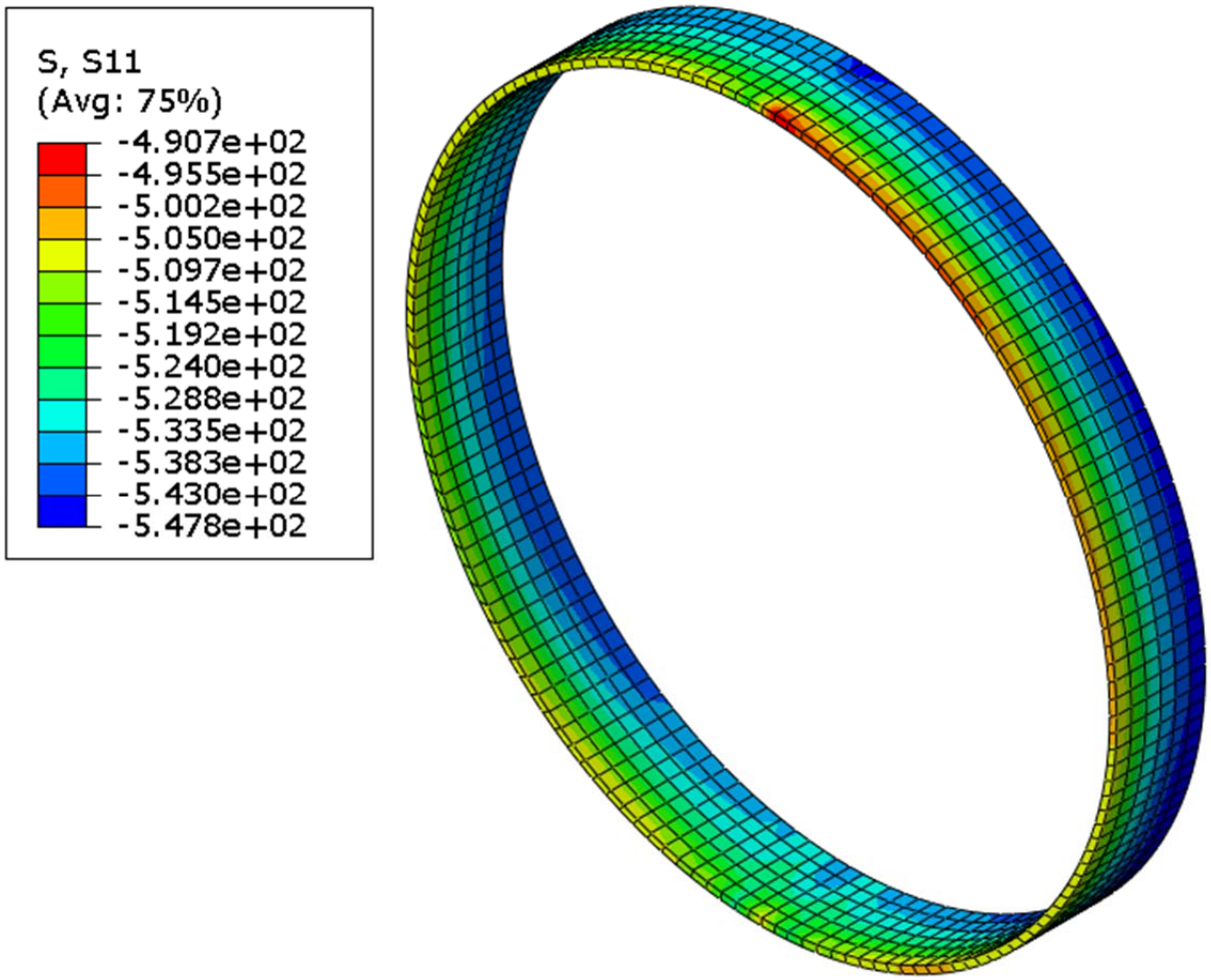

Figure 5.9 Circumferential stress in mortar coating at final prestress

REFERENCES

American Water Works Association. "AWWA C304 Standard for Design of Pre-stressed Concrete Cylinder Pipe." *Denver, CO* (2007).

American Concrete Pipe Association. *Concrete pipe design handbook*. American Concrete Pipe Association, 1987.

American Water Works Association. "Standard for Design of Pre-stressed Concrete Cylinder Pipe." *ANSI/AWWA C301-92* (2007).

Bažant, Zdeněk P., and B_H Oh. "Crack band theory for fracture of concrete." *Matériaux et construction* 16.3 (1983): 155-177.

Bažant, Z. P. "Mechanics of fracture and progressive cracking in concrete structures." *Fracture mechanics of concrete: Structural application and numerical calculation*. Springer Netherlands, 1984. 1-94.

Cedolin, Luigi, Sandro Dei Poli, and Yves RJ Crutzen. "Triaxial stress-strain relationship for concrete." *Journal of the Engineering Mechanics Division* 103.3 (1977): 423-439.

De Borst, R. "Smeared cracking, plasticity, creep, and thermal loading—A unified approach." *Computer methods in applied mechanics and engineering* 62.1 (1987): 89-110.

Diab, Youssef Georges, and Thomas Bonierbale. "A Numerical Modeling and a Proposal for Rehabilitation of PCCPs." *Castronovo J P. Pipelines* (2001).

Gomez, Roberto, et al. "Structural Model for Stress Evaluation of Pre-stressed Concrete Pipes of the Cutzamala System." *Galleher JJ, Stift M T. Pipeline Engineering and Construction: What's on the Horizon* (2004).

Hillerborg, Arne, Mats Modéer, and P-E. Petersson. "Analysis of crack formation and crack growth in concrete by means of fracture mechanics and finite elements." *Cement and concrete research* 6.6 (1976): 773-781.

Lotfi, Hamid R., Ralph G. Oesterle, and John Roller. "Reliability assessment of distressed pre-stressed concrete cylinder pipe." ASCE, 2005.

Lubliner, J., et al. "A plastic-damage model for concrete." *International Journal of Solids and Structures* 25.3 (1989): 299-326.

Manual, A. W. W. A. "M9-99." *Concrete Pressure Pipe*.

Onate, E., et al. "A constitutive model for cracking of concrete based on the incremental theory of plasticity." *Engineering computations* 5.4 (1988): 309-319.

Rashid, Y. R. "Ultimate strength analysis of prestressed concrete pressure vessels." *Nuclear Engineering and Design* 7.4 (1968): 334-344.

Romer, Andrew E. *Failure of prestressed concrete cylinder pipe*. AWWA Research Foundation, 2008.

Romer, Andrew E., Graham EC Bell, and P. E. R Dan Ellison. "Failure of Prestressed Concrete Cylinder Pipe." ASCE, 2007.

Whitlock, Ernest W. "Concrete Pressure Pipe in Today's Water Industry." *Journal (American Water Works Association)* 52.10 (1960): 1244-1250

Zarghamee, Mehdi S., Daniel W. Eggers, and Rasko P. Ojdrovic. "Finite-element modeling of failure of PCCP with broken wires subjected to combined loads." ASCE, 2004.

Zarghamee, Mehdi S., Frank J. Heger, and William R. Dana. "Experimental Evaluation of Design Methods for Pre-stressed Concrete Plpe." *Journal of transportation engineering* 114.6 (1988): 635-655.

Zarghamee, Mehdi S., and W. R. Dana. "A step-by-step integration procedure for computing state of stress in pre-stressed concrete pipe.”." *Computer analysis of the effects of creep, shrinkage, and temperature changes on concrete structures; ACI SP* 129 (1991): 155-170.

BIOGRAPHICAL INFORMATION

Sangit Rauniyar was born in February 19, 1983 in Phattepur VDC-3, Saptari, Nepal. He completed Intermediate in Civil Engineering with first division in 2002 from Institute of Engineering, Western Regional Campus, Tribhuvan University, Nepal. Then, he received his Bachelor's degree in civil engineering with distinction division from Institute of Engineering, Pulchowk Campus, Tribhuvan University, Nepal, which is in first rank in Nepal. He received certificate of appreciation for securing first position in civil engineering entrance examination in Nepal in 2003. Also, He was awarded with Golden Jubilee Scholarship for pursuing Bachelor's degree in Civil Engineering from Embassy of India, Kathmandu, Nepal.

After completing Bachelor's degree, he started working for Radha Structures Pvt. Ltd. as a civil engineer. He immigrated to the United States, and entered the University of Texas at Arlington (UTA) in 2011 to pursue master's degree in civil engineering with major in structural engineering. He did research under Prof. Dr. Abolmaali, a Tseng Huang Endowed Professor of Structural and Applied Mechanics, in finite element modeling of prestressed concrete cylinder pipe. He worked as a research assistant under Dr. Abolmaali in Center for Structural Engineering Research/ Simulation, UTA. He received scholarships for excellent academic performance in UTA. He is working as a design structural engineer for Sabre Tubular Structures, Alvarado, TX.